Breast Cancer: Targets and Therapy

Dovepress
Taylor & Francis Group

Open Access Full Text Article

ORIGINAL RESEARCH

Bystin is a Prognosis and Immune Biomarker: From Pan-Cancer Analysis to Validation in Breast Cancer

Xiyidan Aimaiti[1,2,*], Yiyang Wang[1,2,*], Dilimulati Ismtula[2,*], Yongxiang Li[2], Haotian Ma[2], Junyi Wang[2], Dilraba Elihamu[2], Chenming Guo[1,2]

[1]State Key Laboratory of Pathogenesis, Prevention and Treatment of High Incidence Diseases in Central Asia, The First Affiliated Hospital of Xinjiang Medical University, Urumqi, People's Republic of China; [2]Department of Breast Surgery, Center of Digestive and Vascular, The First Affiliated Hospital of Xinjiang Medical University, Urumqi, People's Republic of China

*These authors contributed equally to this work

Correspondence: Chenming Guo, Email gcm_xjmu@yeah.net

Introduction: The Bystin gene (BYSL) contributes to cancer development and is a probable therapeutic target in cancer therapy. However, no systematic studies have been conducted on BYSL value in pan-cancer diagnosis, prognosis, and immunology.

Methods: We performed a pan-cancer analysis of BYSL using TCGA, GEO, and other databases to assess its expression, clinical significance, genetic variants, methylation, and immune correlation. Enrichment analysis was applied to predict BYSL-related pathways. We analyzed BYSL protein levels in corresponding breast cancer (BRCA) tissue samples to validate our findings using Western blot assays. A tissue microarray was deployed to verify BYSL expression in BRCA tissues by immunohistochemical staining. Moreover, we comprehensively analyzed the function of BYSL in BRCA initiation and development through CCK-8, transwell invasion, migration assays, and cell scratch assays for migration ability assessment.

Results: Through the study, BYSL was significantly overexpressed in the majority of cancers relative to normal tissues, with different expression patterns at different clinicopathological stages. In most cancer types, BYSL exhibits moderate to high diagnostic value, and overexpressed BYSL represents an independent prognosis factor in patients having BRCA, HNSC, KICH, LIHC, OV, and SARC cancers. Mutations in BYSL are distributed in most cancers and are related to prognosis. Most tumors have elevated levels of m6A methylation compared to normal tissues, while their promoter regions exhibit low levels of methylation. Additionally, BYSL expression displayed a positive correlation with MDSC immune infiltration. Further enrichment analysis showed the involvement of BYSL in important biological processes (BP), In addition, BYSL was overexpressed in BRCA tissues and promoted their proliferation, invasion, and migration compared to matched normal breast tissues.

Discussion: Our study showed that BYSL is an important biological indicator for predicting pan-cancer survival outcomes and immune characteristics and elucidated BYSL expression and role in BRCA, which highlights its therapeutic potential in BRCA.

Keywords: pan-cancer, BYSL, prognosis, methylation, tumor immunity

Introduction

Cancer is the primary disease burden that seriously threatens human health,[1,2] due to its complex pathogenesis and diverse biological behaviors, which pose serious challenges to the accurate diagnosis, effective treatment, and prognosis assessment of diseases. Its complexity is largely a result of numerous molecular-level changes within tumor cells and tumor microenvironment (TME) heterogeneity.[3] The rapid development of bioinformatics and molecular biology led to the evolution of biomarkers of great potential in the early diagnosis of cancer, the evaluation of treatment effects, and the prediction of patient prognosis, bringing new hope for the realization of precision medicine for cancer.

BYSL is a gene exhibiting a high conservation degree in the evolution from yeast to humans[4,5] and involves 40S ribosomal subunit biogenesis and 18S pre-rRNA processing.[6] According to research, BYSL may contribute to cancer

Received: 11 June 2025
Accepted: 20 August 2025
Published: 29 August 2025

occurrence and progression. For example, human hepatocellular carcinoma (HCC) specimens have been found to have significantly overexpressed BYSL mRNA and protein levels compared with adjacent tissues, and this expression is essential for nucleation during cancer cell proliferation.[7–9] Moreover, high BYSL expression has been reported to have a close connection to lymph node metastasis, TNM stage, recurrence, and metastasis in osteosarcoma patients and is an independent risk factor affecting their prognosis.[10] BYSL is also involved in the occurrence of BRCA,[11] prostate cancer,[12] gastric cancer,[13] epithelial ovarian cancer,[14] and skin melanoma.[15] In conclusion, the BYSL gene is expected to be a possible biomarker for cancer diagnosis, treatment, and prognosis, as well as a predictor for assessing response to immunotherapy.

Nonetheless, no comprehensive pan-cancer research has been performed on BYSL; therefore, we conducted a systematic bioinformatics analysis based on the existing large number of cancer data and elucidated BYSL expression pattern and biological function in pan-cancer in multiple dimensions, in particular, since the role of BYSL in breast cancer remains unclear, we conducted a variety of experiments to verify its expression and its role in the occurrence and development of breast cancer.

Methods

Differential Expression Analysis of BYSL in Pan-Cancer

By accessing UCSC XENA (https://xenabrowser.net/datapages/), we collected and analyzed clinical data of 33 cancer-associated RNA-seq expression profiles and associated patients (n = 15776) from the TCGA and GTEx databases, converting the data in the transcripts per million (TPM) format using log2 and then combined for further analysis. The "tidyverse" and "reshape" packages were utilized for data collection and cleaning. As for data analysis and visualization, we deployed the R packages "rstatix", "car", and "ggplot2" (v4.4.2).

In addition, we use data from the Comprehensive Gene Expression Database (GEO), including GSE45827 (GPL570), GSE83889 (GPL10558), GSE6791 (GPL570), GSE121248 (GPL570), GSE31547 (GPL96), GSE29450 (GPL570), GSE46517 (GPL96) and GSE54129 (GPL570), to verify BYSL mRNA expression. We also investigated the association of BYSL expression with clinicopathologic features of pan-cancer.

Seeking the verification of BYSL protein level expression, first, we analyzed its protein content and phosphorylation in pan-cancer tissues and their matching normal counterparts by the "CPTAC" module of the UALCAN database.[16] Second, the Human Protein Atlas (HPA) database[17] was accessed to obtain an immunohistochemistry (IHC) Image of BYSL protein expression.

Analysis of BYSL Potential Value in Pan-Cancer Diagnosis and Prognosis

BYSL's potential value in pan-cancer prognosis was ascertained by first conducting Kaplan-Meier analysis (K-M),[18] an online database based on a meta-analysis of gene prognostic values. Second, the interconnection between BYSL expression and prognostic indicators: Overall survival (OS), disease-specific survival (DSS), and progression-free survival (PFS) in pan-cancer patients were explored via each sample survival data in the TCGA. Finally, the "ggplot2" software package generated forest plots and Venn plots to visualize the research results.

The ROC curves were analyzed to assess BYSL predictive value in distinguishing tumor tissue from the corresponding normal tissue. The AUC is a key indicator of diagnostic performance, with values approaching 1 reflecting higher diagnostic accuracy: 0.7–0.9 implies that BYSL possesses moderate diagnostic capability; > 0.9 signifies strong diagnostic potential.

Prognostic Nomogram and Calibration Curve

First, we performed a univariate Cox regression analysis (UCRA), screened out the factors having a $p < 0.1$, and included them in the multivariate Cox regression analysis (MCRA). Subsequently, we incorporated all the factors involved in the MCRA into the prognostic nomogram and determined its predictive validity using the concordance index (C-index). This entire process was repeated 1000 times, thereby plotting a calibration curve to evaluate the consistency of predicted and actual survival outcomes.

Genetic Variant Characterization of BYSL

cBioPortal database,[19] the "OncoPrint" module was used to investigate BYSL genetic variants in the "TCGA Pan-Cancer Atlas Studies" dataset, which included 10443 mutation data from 32 studies (n = 10,967). The "Cancer Types Summary" module was used to assess BYSL gene mutation number, mutation types, and copy number variants (CNV) in each malignancy. The "mutation" module is employed to evaluate mutation sites of BYSL and display them in its protein 3D structure.

The "Mutation-CNV" module of GSCA[20] was deployed to explore CNV percentage in pan-cancer and the interconnection between BYSL mRNA levels and CNV in pan-cancer. In addition, we explored CNV's impact in BYSL on cancer patients' prognosis.

Utilization of Online Databases

The UALCAN database "TCGA" module was used for the comparison of BYSL promoter methylation levels in normal and pan-cancer samples. Additionally, we deployed the GSCA database module "Mutation-Methylation" to explore the influence of BYSL promoter methylation levels on pan-cancer patients' prognosis (OS, PFS, DSS).

Here, the connection between BYSL gene levels and tumor mutational burden (TMB), microsatellite instability (MSI), and neoantigen (NEO) was examined in diverse malignancies via the Sangerbox3.0[21] online database. Then, the "estimate" package was employed to calculate the interaction between BYSL mRNA levels and tumor stromal, immune invasion, and tumor purity scores.

The ssGSEA was utilized to evaluate the interconnection between BYSL mRNA levels and 24 immune cells (IC) infiltration levels in pan-cancer. The TIMER, EPIC, MCPCOUNTER, QUANTISEQ, and XCELL algorithms of the TIMER 2.0 "Immune" module[22] were utilized to evaluate the link between BYSL mRNA levels in pan-cancer and IC infiltration levels: CD8+/CD4+ T cells, regulatory T cells (Treg), B cells, and cancer-associated fibroblast (CAFs).

Fifty experimentally validated BYSL-binding proteins were obtained via the STRING database,[23] and a protein-protein interaction (PPI) diagram was built for visualization. The GEPIA2 database[24] was accessed to retrieve the first 100 co-expressed genes of BYSL. We started by plotting a Venn diagram to identify genes common to the BYSL-binding protein and associated genes. Thereafter, the connection between BYSL and these genes was investigated by the TIMER 2.0 database. The "cluster Profiler" and "ggplot2" packages were used for BYSL functional enrichment analysis and result visualization. The bubble chart shows only the top five items that are most associated with tumors in each type.

Furthermore, we divided the expression of BYSL into high- (HEG) and low-expression groups (LEG), with 50% as the threshold. The "DESeq2" package was utilized to conduct differential expression analysis on individual genes. All genes and their corresponding "log2FoldChange" values were incorporated into the GSEA. To clarify the functional differences between the HEG and LEG in the pan-cancer cohort, we adopted the MSigDB "c2.cp.v7.2.symbols.gmt" gene set[25] and repeated the operation 10,000 times, visualizing the top ten "Reactome pathways" for each tumor in a ridge diagram.

Patient Tissue Sample Collection

In this study, cancer tissues and adjacent tissues of 16 BRCA patients who received surgery in the Department of Breast Surgery, the First Affiliated Hospital of Xinjiang Medical University from January 2024 to December 2024 and strictly met the inclusion and exclusion criteria (not receiving radiotherapy, chemotherapy, and hormone therapy before surgery) were collected. Patients signed informed consent before surgery, which was reviewed and authorized by the Ethics Committee of the same organization (No.230714–08). All fresh samples were snap-frozen in liquid nitrogen and frozen in a –80 °C freezer immediately after surgical resection before qRT-PCR and Western blotting (WB).

Plasmid Construction and Transfection

Construction of BYSL knockdown vector (sh-BYSL): Three sequences of specific small hairpin RNA (shRNA) (Supplementary Table S1) were selected to knock down BYSL expression, and the shRNA was inserted into the polyclonal site (MCS) of the lentiviral vector GV493. Cloning was performed by restriction enzyme digestion and

ligation reactions, and the constructed plasmids were verified by DNA sequencing. Construction of BYSL overexpression vector: Lentiviral vector GV385 was used to insert the BYSL gene into the appropriate position and select the appropriate promoter to drive the expression of BYSL. The constructed vector was confirmed by DNA sequencing.

The constructed shRNA or overexpression plasmid (2 μg) was mixed with the transfection reagent Lipofectamine 3000 (Invitrogen, Shanghai, China) based on the proportion indicated by the reagent and transfected into HEK-293T cells that grew to about 80%. The cells were cultured for 48 h to allow virus particles to be produced, thereby collecting, filtering, and concentrating the supernatant by ultrafiltration (100,000 x g, 4 °C, 2 h). After ultrafiltration, the supernatant was discarded, and the pellet was resuspended in a medium.

Lentivirus Infection and Grouping

BRCA cell lines HCC-1937 and MDA-MB-231 were inoculated in the plates, and virus infection was performed when the cells grew to about 80%. The concentrated lentivirus solution was introduced to the cells, which were replaced with fresh culture medium 24 h after infection and continued to be cultured for 48 h. According to the above methods, the cells were divided into three groups: BYSL knockdown empty vector group; BYSL knockdown group (BYSL-KD); BYSL overexpression vector group; BYSL overexpression group (BYSL-OE); There were four groups. The expression of genes was observed by fluorescence microscopy 72 h post-infection, culturing the cells in good condition for a period and collected for subsequent experiments.

RNA Extraction and qRT-PCR

Following the protocols, we extracted total RNA by Trizol (Invitrogen, Shanghai, China) via the SYBR Green PCR kit (Takara, Kyoto, Japan). Furthermore, forward and reverse primers (Table S1) were used to amplify the target genes in a 20 μL final volume. The qRT-PCR reaction process was performed in Applied Biosystems 7500 (Foster City, CA, USA), and data were analyzed with the $2^{-\Delta\Delta CT}$ method.

Protein Extraction and WB

Per the protocols, the collected tissues and cells were used for total protein extraction using RIPA lysate containing PMSF protease inhibitor, and the BRCA protein assay kit (all from Beyotime, Shanghai, China) was employed for total protein extraction to determine protein concentration. The protein samples were loaded onto a 10% SDS-PAGE gel to separate the total proteins, transferred to a PVDF membrane, blocked, and incubated with the primary antibody BYSL (ab251811, Abcam, USA) at 4 °C. β-Actin (Sc-69879, Santa Cruz Biotechnology, USA) was incubated overnight as a loading control. Secondary antibodies containing horseradish peroxidase were incubated for 1 h at room temperature and then dipped in ECL chemiluminescence reagent (both from Cell Signaling Technology, USA, USA). Massachusetts, USA) were then recorded using a Bio-Rad imaging system.

IHC Staining

The human tissue microarray chip used in this study contained 80 pairs of BRCA and paracancer tissues (BRC1603, Superbiotek, Inc., Shanghai, China). Standard IHC staining was applied on tissue microarray slides using a protein-specific anti-BYSL antibody (ab251811, Abcam, USA) after heat repair using citrate buffer pH = 6.0 (Invitrogen, Shanghai, China). Two pathologists evaluated the staining results in a blinded method, and each tissue sample was scored based on its staining intensity (none = 0; Weak = 1 point; Medium = 2; Strong = 3) multiplied by stained cell percentage (Positive rates ≤ 25% = 1 point; 26–50% = 2; 51–75% = 3; ≥ 75% = 4) were calculated as 0–12 points: 0–5 points, low expression; 6–12 points, high expression.

CCK-8 Assay

The cell viability assay kit (CCK-8; Dojindo Molecular Technologies, Japan) was deployed for cell proliferation ability assay by seeding cells in 96-well plates and cultured for five days. This was followed by introducing CCK-8 reagent to each well and incubated at 37 °C for 1.5 h. Subsequently, the absorbance value at 450 nm was measured in a microplate

reader (Tecan Infinite, Switzerland). The measured results were plotted as a discount plot to reflect changes in cell proliferation capacity.

Transwell Assay

A Transwell assay kit (Corning, New York, USA) was deployed to inoculate the cells in the experimental and control groups, respectively. Cell invasion and migration assays were conducted in the transwell chamber with or without Matrigel. Transwell chambers inserted with 600 μL of 10% FBS medium were placed in the lower chamber as a chemoattractant and incubated for 24 h at 5% CO_2 and 37 °C. Residual cells on the membrane surface of the inserted object were eliminated by a cotton swab. The total cell number that invaded the lower chamber was then fixed with 4% paraformaldehyde for half an hour before being stained with 0.1% crystal violet (both from Beyotime, Shanghai, China). Cells were examined and quantified with an inverted microscope (Mshot, Guangzhou, China) at 200× magnification.

Oris Cell Migration Assay

First, the OrisTM blockage was soaked in alcohol, sterilized, dried, and placed in a 96-well plate. The infected cells were added to the wells according to the designed group, and it was advisable to reach 90% the next day. The OrisTM blockage was carefully removed the next day, Celigo continued to culture after scanning the plate, and the cell area was calculated by taking photos at the appropriate time (0, 24 h). Cell mobility was assessed by calculating the difference in cell area at different time points. The cell mobility rate was determined using the formula: (0 h blank area − 24 h blank area)/0 h blank area × 100%.

Statistical Analysis

Statistical analyses were conducted through R software (v4.4.1), visualizing the data with the "ggplot2" package. Using the BYSL mRNA median level, the samples were allocated into HEG and LEG. For the difference in BYSL expression levels in unpaired samples, we employed the Mann–Whitney *U*-test to detect the difference while using the Wilcoxon signed-rank test for paired samples. The Spearman correlation coefficient was deployed to ascertain the link between BYSL expression and m6A methylation regulators, TMB, MSI, NEO, immune scores, and immune-associated genes. $P < 0.05$ indicated statistical significance: $*p < 0.05$; $**p < 0.01$; $***p < 0.001$; NS, Not Significant.

Results

Differential Expression of BYSL in Diverse Human Cancers

We used TCGA, GTEx, and GEO data to investigate the expression of BYSL mRNA in tumor and normal tissues. The TCGA database results manifested that BYSL expression was higher in 16 tumors (BLCA, BRCA, CHOL, COAD, ESCA, GBM, HNSC, KIRC, KIRP, LIHC, LUAD, LUSC, PRAD, READ, STAD, and UCEC) while being lower in KICH than in the corresponding normal tissues (normal samples were obtained from healthy individuals) (Figure 1A).

Besides, GTEx normal tissues were matched to TCGA cancer tissues, showing that BYSL was significantly over-expressed in 25 cancers (BLCA, BRCA, CHOL, COAD, ESCA, GBM, HNSC, KIRC, KIRP, LIHC, LUAD, LUSC, PRAD, READ, STAD, UCEC, CESC, DLBC, LGG, OV, PAAD, SKCM, TGCT, THYM, and UCS) and suppressed in KICH and LAML relative to healthy tissues ($p < 0.001$; Figure 1B).

Moreover, research on paired samples of 23 cancers found that BYSL was significantly overexpressed relative to the corresponding matched normal tissues in 15 malignancies (BLCA, BRCA, CHOL, COAD, ESCA, HNSC, KIRC, KIRP, LIHC, LUAD, LUSC, PRAD, READ, STAD, UCEC) ($p < 0.01$; Figure 1C). To be more convincing, we further validated our findings using datasets from the GEO database, specifically in BRCA, COAD, HNSC, LIHC, LUAD, OV, SKCM, and STAD, BYSL mRNA displayed higher levels than matched normal tissues ($p < 0.01$; Figure 1D–K). The Clinicopathologic features of pan-cancer from the TCGA database showed that BYSL was significantly overexpressed with pathological stage progression in cancers such as ACC, KIRP, LIHC, and LUAD, among others, implying that BYSL may be a prognostic marker for these cancers. In contrast, BYSL was significantly elevated in patients with early

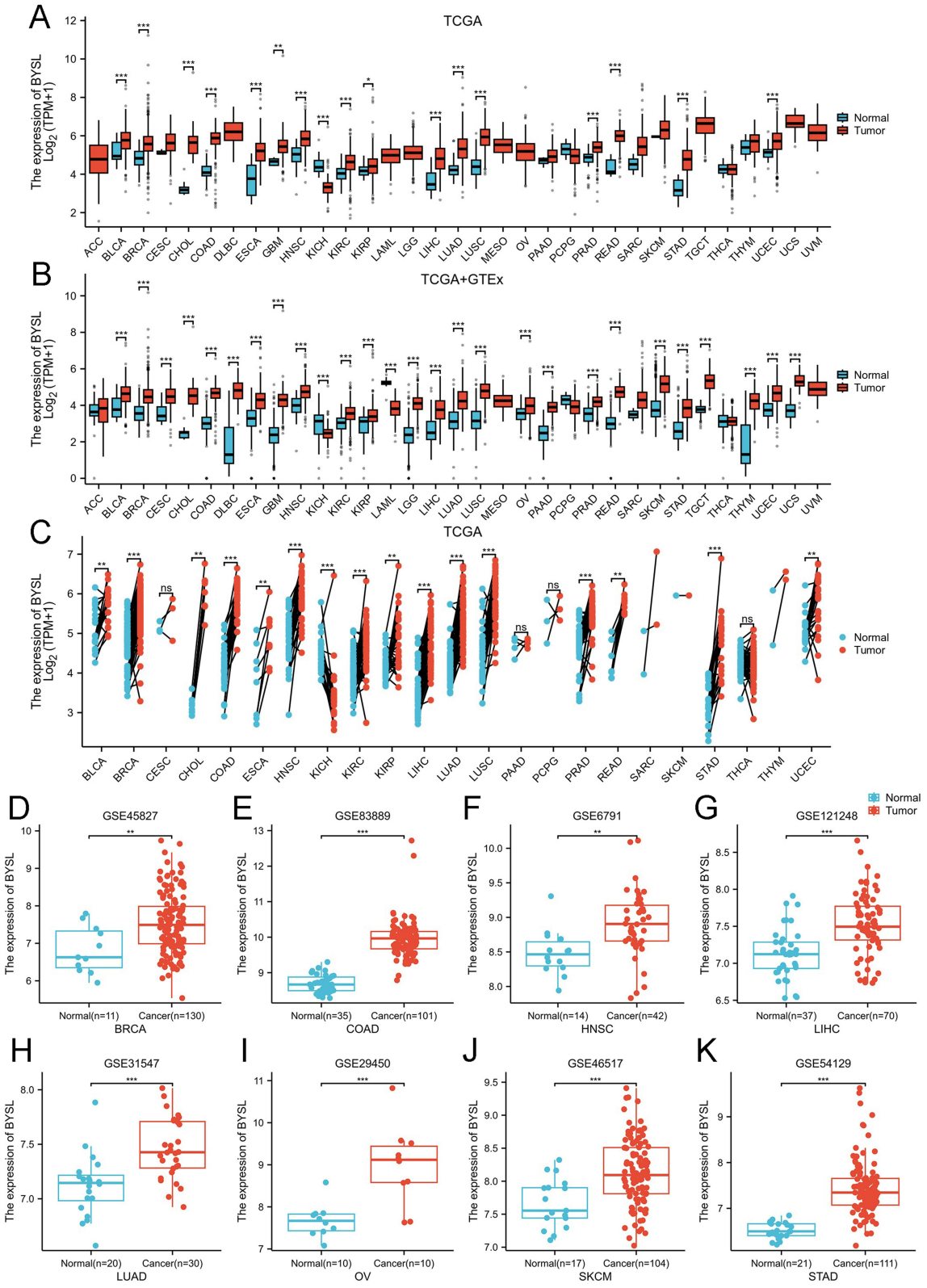

Figure 1 BYSL mRNA expression levels across 33 cancers. (**A**) BYSL mRNA levels in TCGA tumor and corresponding normal tissue. (**B**) Integration of TCGA and TCGA-GTEx for comparison of BYSL mRNA expression differences in normal and tumor tissues. (**C**) BYSL mRNA level in TCGA tumor samples vs paired normal tissues. GEO datasets: BYSL expression differences for specific cancers. (**D**) BRCA (GSE45827), (**E**) COAD (GSE83889), (**F**) HNSC (GSE6791), (**G**) LIHC (GSE121248), (**H**) LUAD (GSE31547), (**I**) OV (GSE29450), (**J**) SKCM (GSE46517), and (**K**) STAD (GSE54129). (*$p < 0.05$, **$p < 0.01$, ***$p < 0.001$, NS-Not Significant).

https://doi.org/10.2147/BCTT.S537429

OV and SKCM. Moreover, the expression level decreased with tumor progression, suggesting that BYSL expression may have potential value for early OV and SKCM diagnosis (Supplementary Figure S2A–F).

The results of the UALCAN database revealed high BYSL protein levels in BRCA, COAD, KIRC, UCEC, lung cancer, HNSC, glioblastoma, and liver cancer compared to normal tissues (Figure 2A). At the same time, changes in protein phosphorylation levels were found in BRCA, HNSC, KIRC, COAD, LIHC, LUAD, LUSC, OV, PAAD, and the most critical site of phosphorylation was NP-004044.3:S98, followed by NP-004044.3:S167. There are the most phosphorylation sites in COAD. Phosphorylation levels are reduced at most phosphorylation sites in COAD, OV, and PAAD compared to healthy tissues (Figure 2B).

The results of IHC obtained from the HPA dataset demonstrated that BYSL protein was significantly increased in BLCA, BRCA, COAD, HNSC, LIHC, LUAD, LUSC, OV, PRAD, RCC, SKCM, and UCEC compared to normal tissues, which was similar to the previous BYSL mRNA expression is consistent in pan-cancer (Supplementary Figure S1).

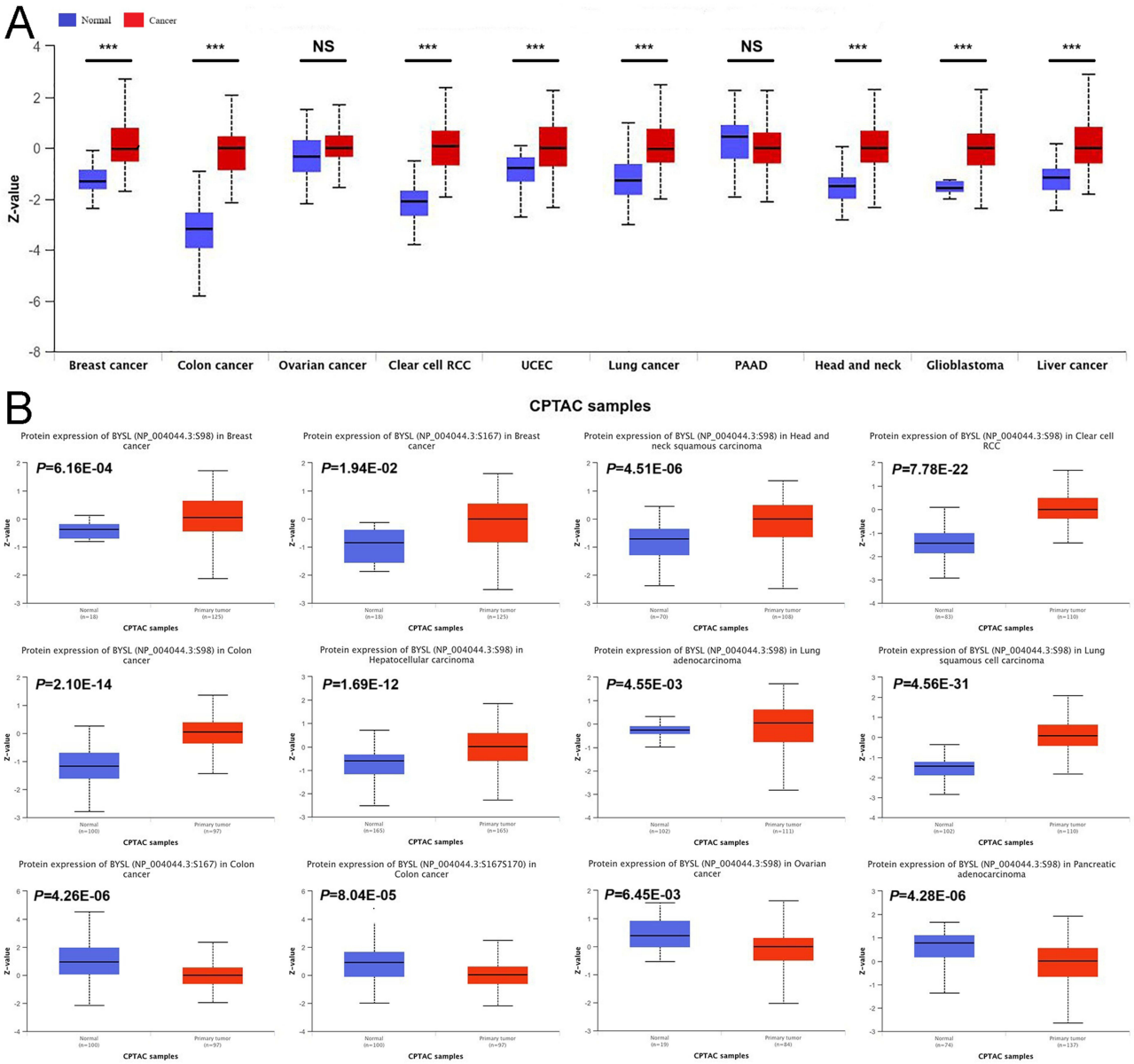

Figure 2 Expression of BYSL. (**A**) BYSL protein expression levels across tumor and normal samples. (**B**) BYSL protein level and phosphorylation sites in various cancers. (*$p < 0.05$, **$p < 0.01$, ***$p < 0.001$, NS-Not Significant).

https://doi.org/10.2147/BCTT.S537429

Collectively, BYSL mRNA expression was significantly upregulated in most cancers, supported by protein-level data. In addition, BYSL mRNA expression is related to clinicopathologic features in multiple cancers, which further demonstrates BYSL's potential significance as a pan-cancer marker.

BYSL Diagnostic and Prognostic Value in Pan-Cancer

The K-M analysis on the impact of BYSL mRNA levels on patients' prognosis with BRCA, LAML, LUAD, STAD, and OV consistently suggests that higher BYSL mRNA expression is connected with a worse prognosis in most cancers (except for OV) ($p < 0.001$; Supplementary Figure S2G). This affects multiple survival indicators, such as OS, DSS, and PFS, among others ($p < 0.001$; Supplementary Figure S3).

In the TCGA database, BYSL prognostic value in OS, DSS, and PFS in pan-cancer patients was studied. BYSL was highly expressed in ACC ($p = 0.008$, hazard ratio (HR) = 3.058), BRCA ($p = 0.004$, HR = 1.605), COAD ($p = 0.026$, HR = 1.569), KIRP ($p = 0.028$, HR = 2.014), LAML ($p = 0.008$, HR = 1.782), LUAD ($p = 0.028$, HR = 1.386), LIHC ($p = 0.028$, HR = 1.477), SARC ($p < 0.001$, HR = 2.260), SKCM ($p = 0.011$, HR = 1.424) and especially in KICH ($p = 0.046$, HR = 8.309), which reduced the OS of patients. In contrast, in THYM ($p = 0.029$, HR = 0.160), BYSL overexpression positively affected patient survival. In conclusion, BYSL overexpression was identified as an OS risk factor in most cancer patients (Figure 3A).

By DSS analysis, we found that in ACC ($p = 0.013$, HR = 2.880), COAD ($p = 0.007$, HR = 2.061), BRCA ($p = 0.002$, HR=1.993), HNSC ($p = 0.005$, HR = 1.657), LUAD ($p = 0.049$, HR = 1.449), SARC ($p = 0.001$, HR = 2.146, SKCM ($p = 0.010$, HR = 1.438), UCEC ($p = 0.030$, HR = 1.726), and especially in KIRP ($p < 0.001$, HR = 9.146) the increase in BYSL expression predicted a worse prognosis for DSS. For OV ($p = 0.047$, HR = 0.752), high expression of BYSL was a favorable factor for patients displaying longer DSS (Figure 3B). Similarly, BYSL overexpression represented an adverse factor impacting PFS in patients having ACC ($p = 0.003$, HR = 2.776), BRCA ($p = 0.008$, HR = 2.880), COAD ($p = 0.017$, HR = 1.538), HNSC ($p = 0.005$, HR = 1.509), KICH ($p = 0.044$, HR = 4.825), KIRP ($p = 0.003$, HR = 2.293), LIHC ($p = 0.005$, HR = 1.520), SARC ($p = 0.015$, HR = 1.508), and UCEC ($p = 0.012$, HR = 1.564), and a favorable factor affecting PFS in OV patients ($p = 0.007$, HR = 0.722) (Figure 3C). The Venn diagram results depicted that BYSL expression affected OS, PFS, and DSS in patients with ACC, BRCA, COAD, KIRP, and SARC. This implies that BYSL may be a key factor influencing their prognosis (Figure 3D). Altogether, BYSL overexpression exhibits a close relation to the poor prognosis of patients with various cancers, and BYSL may be a promising biomarker in predicting pan-cancer patients' prognosis.

Second, the ROC curves results showcased that BYSL showed good diagnostic value (AUC > 0.9) in COAD (0.972), KICH (0.932), LUAD (0.900), LUSC (0.941), READ (0.983), and STAD (0.960), especially in CHOL (1.000) (Figure 4A). BYSL demonstrated moderate diagnostic ability (AUC > 0.7) in multiple cancers, including BRCA (0.835), ESCA (0.898), GBM (0.886), HNSC (0.861), LIHC (0.892), PRAD (0.840), SARC (0.846), BLCA (0.756), CESC (0.771), KIRC (0.781), PAAD (0.703), and UCEC (0.766) (Figure 4B).

Collectively, BYSL overexpression has an interconnection to poor prognosis in multiple cancers and has demonstrated moderate-strong diagnostic power in most cancers.

BYSL Is an Independent Factor Influencing Certain Cancer Prognoses

To comprehend the effects of diverse factors on PFI in cancer patients, we performed Cox regression analyses for ten cancers (ACC, BLCA, COAD, HNSC, KICH, KIRP, LIHC, OV, SARC, and UCEC). For ACC, the MCRA results showed that the Primary therapy outcome (partial response (PR)/complete response (CR), HR = 0.133, $p < 0.001$) was the only independent prognostic factor (PF) (Supplementary Table S2A). For BRCA, the independent predictive variables were pathological M1 stage (HR = 4.679, $p < 0.001$), pathological III/IV stage (HR = 1.847, $p = 0.040$), and BYSL expression (high, HR = 1.522, $p = 0.044$) (Supplementary Table S2B). For COAD, PR/CR (HR = 0.203, $p < 0.001$) represented the only independent predictive variable (Supplementary Table S2C). For HNSC, pathological T3/T4 stage (HR = 1.974, $p < 0.001$) and BYSL level (high, HR = 1.485, $p < 0.019$) represented independent PFs (Supplementary Table S2D). For KICH, pathological T3/T4 stage (HR = 8.326, $p = 0.002$) and BYSL levels (high, HR = 4.797, $p = 0.045$) represented independent PFs (Supplementary Table S2E). For KIRP, gender (female, HR = 2.500,

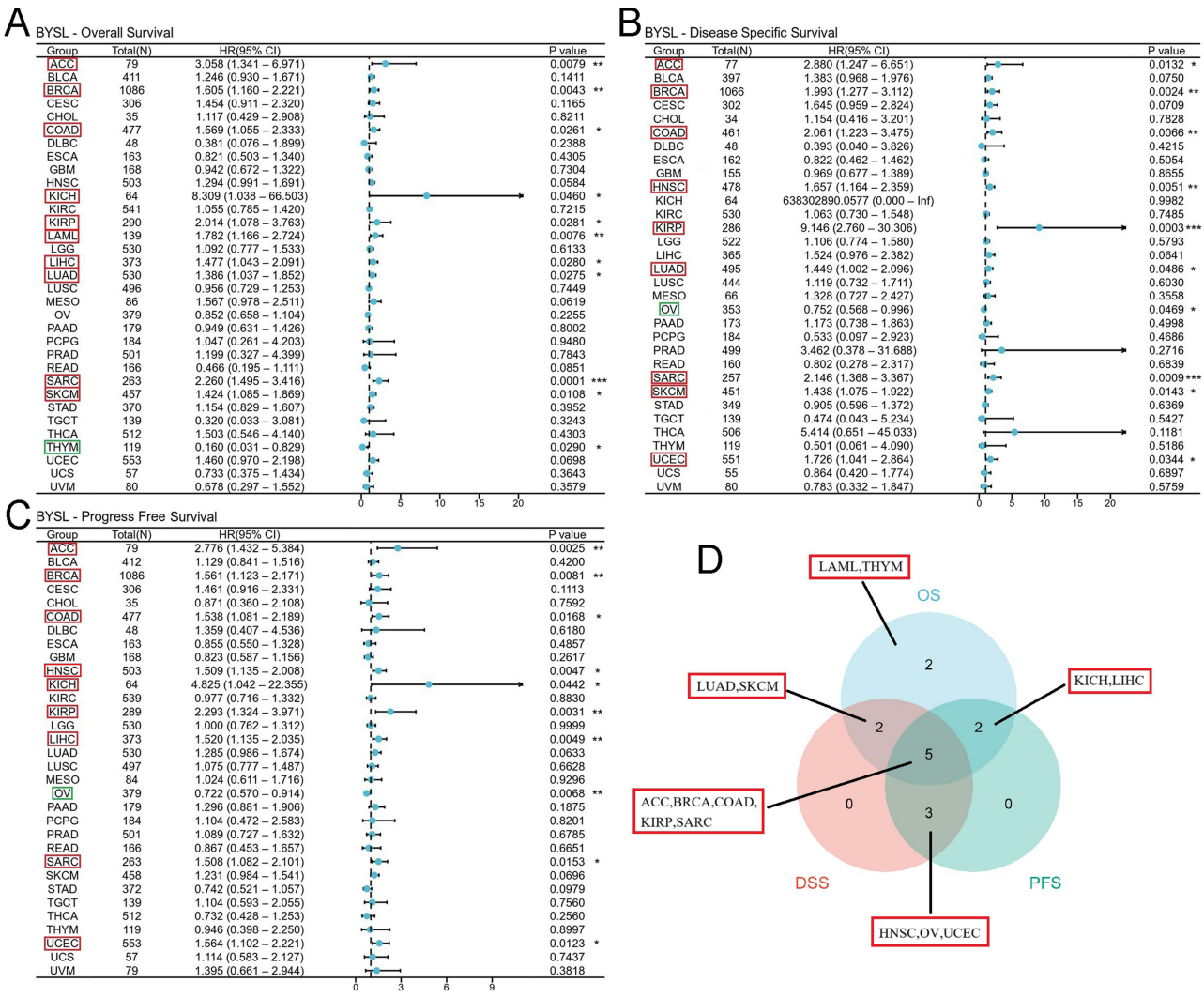

Figure 3 Interaction between BYSL expression and cancer patients prognosis. Interconnection between BYSL expression and (**A**) OS, (**B**) DSS, (**C**) PFS. (**D**) Venn diagram: Intersection of OS, DSS, and PFS for diverse cancers. (*p < 0.05, **p < 0.01, ***p < 0.001, (**A**–**C**) red boxes: High expression of BYSL was a risk factor, green boxes: High expression of BYSL was a favorable factor).

p = 0.047) and clinical III/IV stage (HR = 8.956, p = 0.012) represented independent PFs (Supplementary Table S2F). For LIHC, the BYSL level (high, HR = 1.550, p = 0.015) represented the only independent PF (Supplementary Table S2G). For OV, PR/CR (HR = 0.588, p = 0.004) and BYSL levels were independent predictors (Supplementary Table S2H). In addition, for SARC, Residual tumor R1 (HR = 4.139, p = 0.001), R2 (HR = 8.193, p = 0.007), Tumor Focal necrosis (HR = 5.205, p < 0.001), Tumor Moderate necrosis (HR = 2.209, p = 0.019), Metastasis (yes, HR = 12.464, p < 0.001), and BYSL level (high, HR = 1.764, p = 0.044) were independent PFs (Supplementary Table S2I). For UCEC, PR/CR (HR = 1.764, p = 0.044), clinical III/IV stage (HR = 2.902, p < 0.001), and endometrioid (Mixed, HR = 3.741, p = 0.002) represented independent predictors (Supplementary Table S2J).

Subsequently, we incorporated all the factors involved in the MCRA into the prognostic nomogram, showing that the prognostic nomogram C-index for ACC was 0.804, for COAD was 0.773, for UCEC was 0.751, for BRCA was 0.700, for SARC was 0.845, for OV was 0.622, for LIHC was 0.648, for KICH was 0.817, for KIRP was 0.827, and for HNSC was 0.701 (Figure 5A–H, Supplementary Figure S4A and B). In addition, the calibration curves showed that ten types of cancer approached the ideal line (Supplementary Figure S4C–L). Accordingly, BYSL expression can be an independent predictive variable for the prognosis of patients with these cancers.

https://doi.org/10.2147/BCTT.S537429

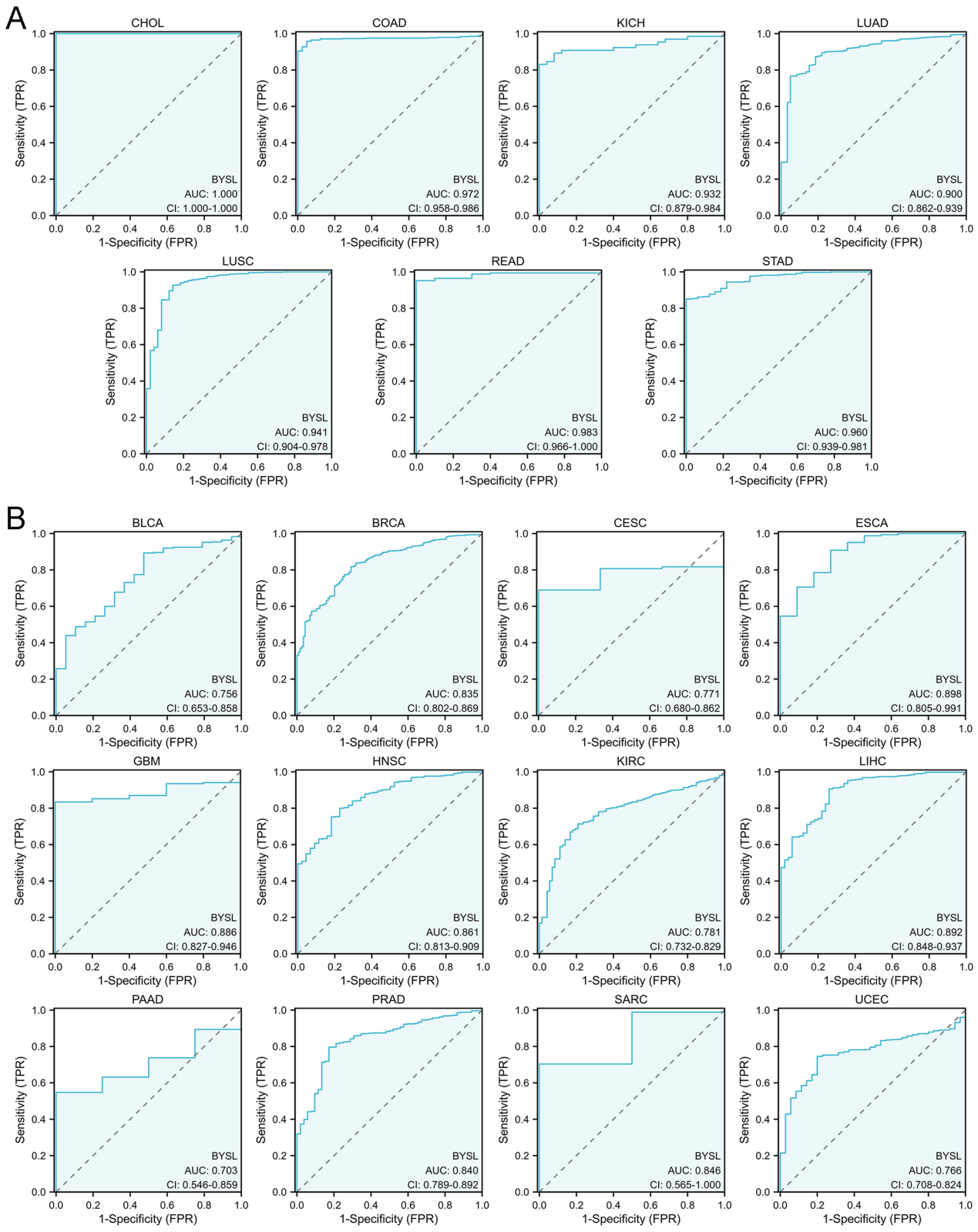

Figure 4 ROC curve for BYSL expression in pan-cancer. (**A**) BYSL expression in CHOL, COAD, KICH, LUAD, LUSC, READ, and STAD cancers with good diagnostic value (AUC > 0.9) as well as (**B**) in BLCA, BRCA, CESC, ESCA, GBM, HNSC, KIRC, LIHC, PAAD, PRAD, SARC, UCEC cancers with some diagnostic value (AUC > 0.7).

Genetic Variant Characterization of BYSL in Pan-Cancer

Genetic mutations can cause cells to lose their regulation of survival, proliferation, and spread, and some of these genetic alterations are potential targets for molecular therapeutics.[26] To explore whether BYSL can be a molecular therapeutic target, we performed a genetic characterization analysis. We found that among 10,967 samples, 253 samples (accounting for 2.3%) had BYSL mutations. Amplification was the most common CNV mutation, then Missense Mutation, Truncating Mutation, and Deep Deletion (Figure 6A). Among them, the proportion of missense mutations is 53.51%, and that of synonymous substitutions is 16.24% (Supplementary Figure S5A). Additionally, the most dominant single nucleotide variant (SNV) category was C>T (39.90%), then G>A (26.77%) (Supplementary Figure S5B). Subsequently, the BYSL gene mutation status was studied in pan-cancer. Among various cancer types, STAD (6.82%), ESCA (6.59%), OV (4.79%), DLBC (4.31%), and SARC (4.28%) exhibited the highest mutation frequencies (Figure 6B). R406W/Q was the most frequently mutated locus in the BYSL domain, and the mutations occurred in one patient with LUSC (R406Q), one SKCM (R406W), and one COAD (R406W), respectively (Figure 6C). Figure 6D shows the mutation status within the BYSL protein 3D structure and sequence.

The GSCA database results manifested that the CNV pie chart derived from this database showed that most cancers showed heterozygous amplification and deletion, homozygous amplification. Rare homozygous deletions occasionally occur in OV, BRCA, LUSC, CESC, AND PRAD (Supplementary Figure S5C). Moreover, BYSL expression is positively related to CNV alternation in most cancers (Supplementary Figure S5D). CNV in BYSL is a detrimental factor impacting patients' prognosis with GBM, KIRP, LGG, LIHC, SARC, UCEC, and UVM (Figure 6E). In conclusion, genetic alterations of BYSL occur in most malignancies and are connected with the poor prognosis of cancer patients. Meanwhile, the genetic alterations of BYSL are expected to serve as potential targets for molecular therapy.

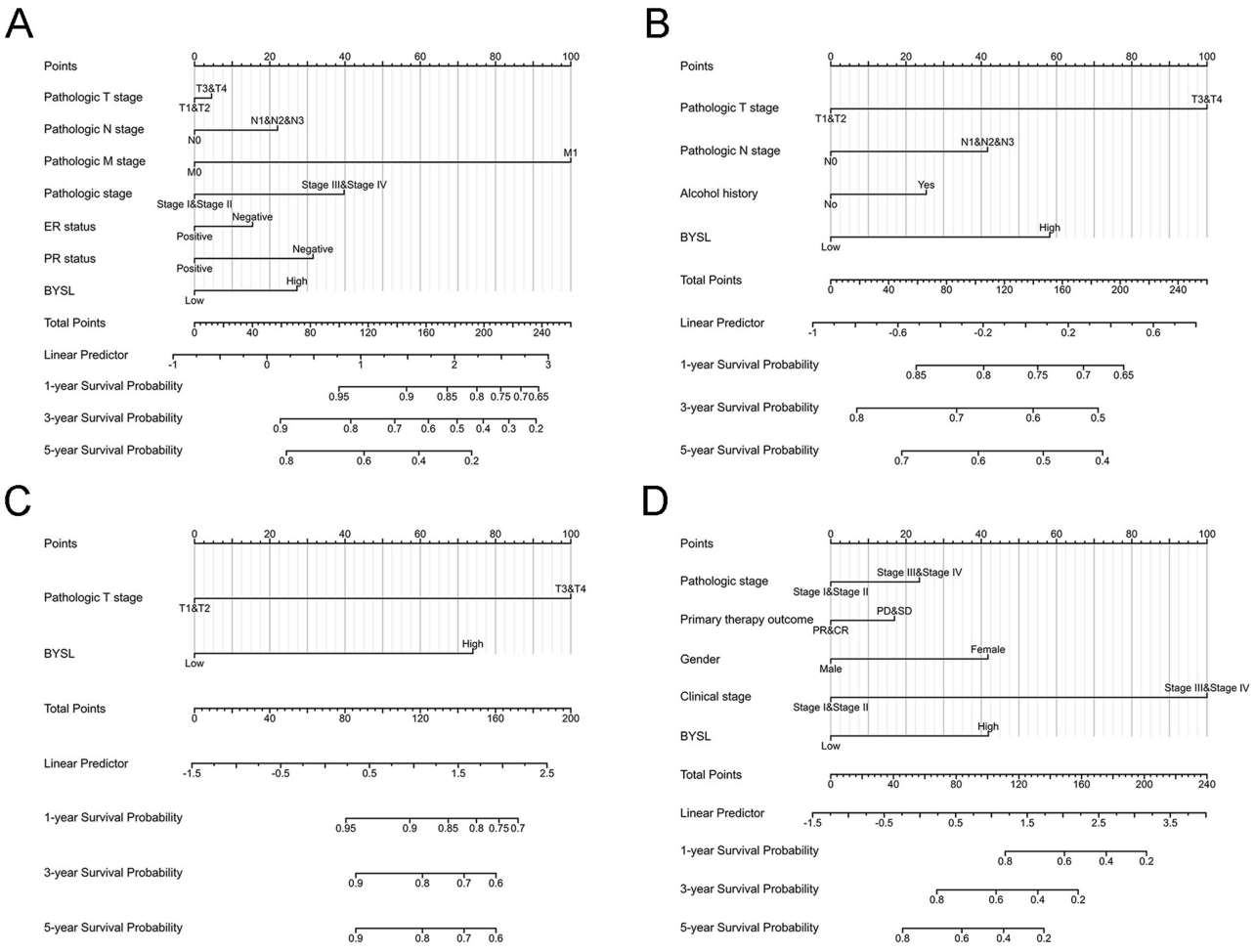

Figure 5 Continued.

https://doi.org/10.2147/BCTT.S537429

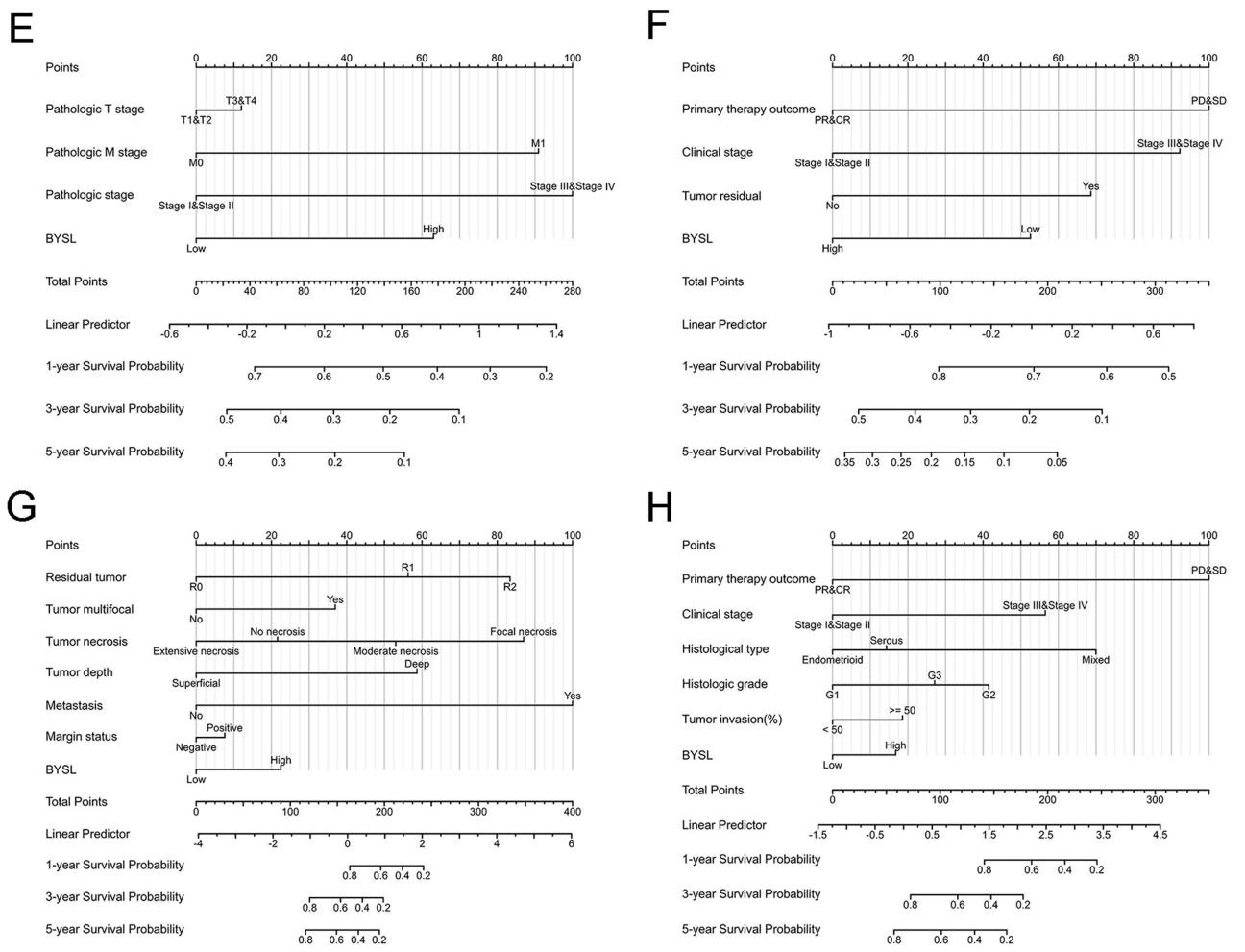

Figure 5 Nomograms prediction of patient PFS in eight cancers. Nomograms for BRCA (**A**), HNSC (**B**), KICH (**C**), KIRP (**D**), LIHC (**E**), OV (**F**), SARC (**G**), and UCEC (**H**).

Exploration of the Association Between BYSL and Methylation

DNA methylation constitutes a key component of gene regulation. Cancer is defined by abnormal DNA methylation, which can promote tumorigenesis and modulate immune responses.[27] As the most abundant and dynamic modification in RNA, m6A holds greater research value in disease progression. Particularly in cancer, abnormal m6A modifications are directly associated with various malignant phenotypes. Therefore, we delve into the interconnection between BYSL expression and key m6A methylation regulators in some cancers. There are 24 m6A methylation regulators: 10 writers (CBLL1, METTL14/3, RBM15/15B, TRMT6/61A/61B, WTAP, and ZC3H13), 3 erasers (FTO and ALKBH3/5), and 11 readers (HNRNPA2B1, HNRNPC, IGF2BP1/2/3, RBMX, and YTHDC1/C2/F1/F2/F3). Heatmaps showed that in most tumors, BYSL expression was positively related to m6A methylation regulator expression (Figure 7A). Given the high expression of BYSL in most cancers from previous studies, it may also exhibit high m6A methylation levels.

The UALCAN database research showed that unlike normal tissues, the BYSL promoter was hypomethylated in BLCA (p = 2.91E-12), BRCA (p = 2.48E-07), CESC (p = 2.88E-02), HNSC (p = 1.62E-12), LIHC (p < 1.00E-12), LUAD (p = 1.34E-09), LUSC (p = 3.67E-09), PRAD (p = 8.36E-12), READ (p = 3.90E-07), TGCT (p = 2.40E-11), THCA (p = 1.04E-02), UCEC (p < 1.00E-12). In contrast, it was hypermethylated in KIRC (p = 1.06E-03) and KIRP (p = 4.21E-05) (Figure 7B). Subsequently, the influence of BYSL methylation level on cancer patient's prognosis, including OS, PFS, and DSS, was analyzed, revealing that BYSL hypermethylation status is a BLCA risk factor and KIRC protective factor (Supplementary Figure S5E).

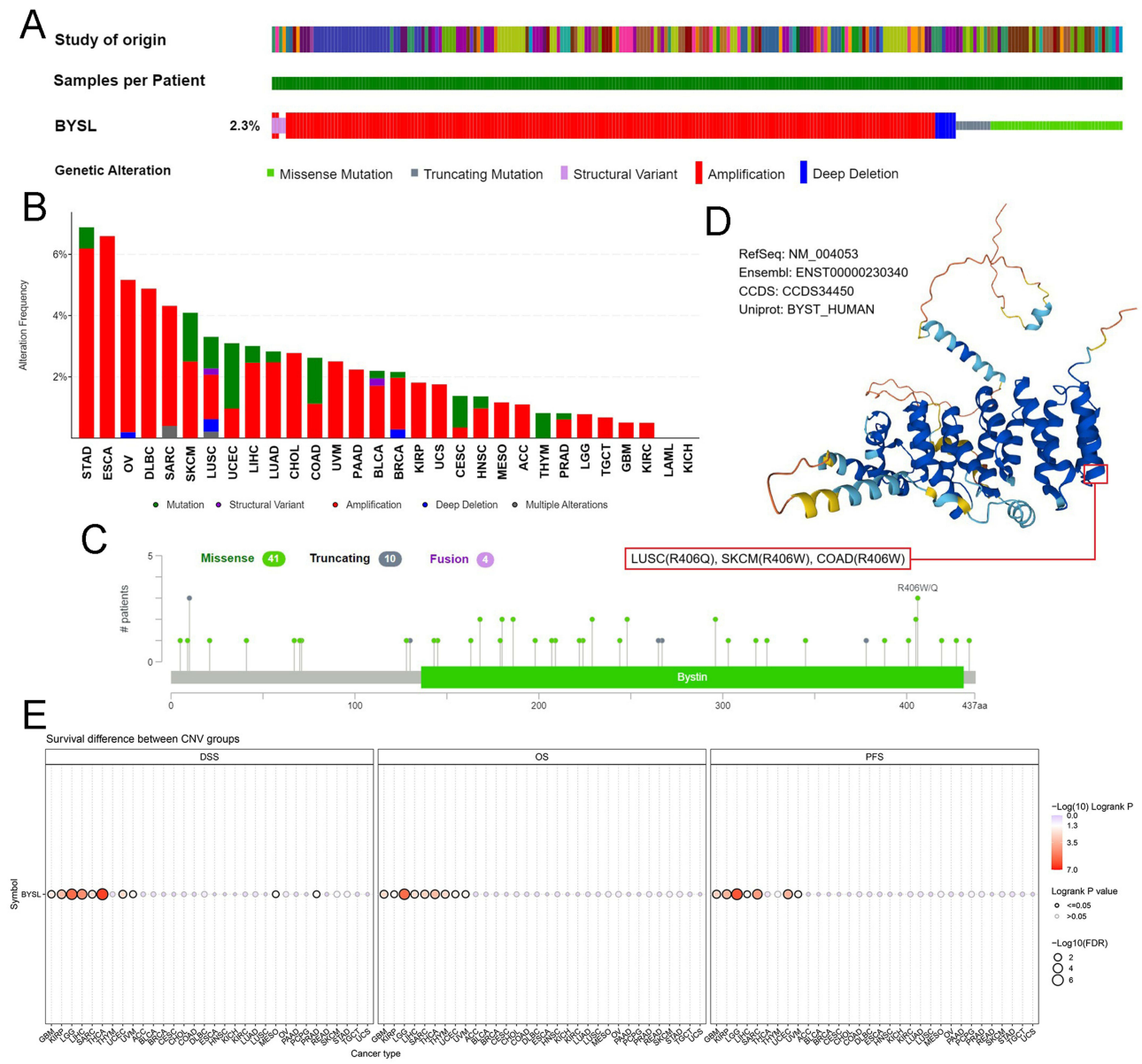

Figure 6 Mutational landscape of BYSL in cancer. (**A**) Expression alterations across tumors. (**B**–**C**) Mutation distribution and mapped sites. (**D**) 3D structural view of key mutations. (**E**) Prognostic impact of BYSL CNVs.

Altogether, BYSL is overexpressed in most malignancies and is positively related to most m6A methylation-related gene expression. Based on this, we speculate that BYSL exhibits a high methylation level in most tumors, and this methylation level has an impact on cancer patients' prognosis.

Correlation Analysis Between BYSL Expression and Immunity

Studies have shown that TMB, MSI, and NEO serve as predictive biomarkers that can predict response to immunotherapy. Accordingly, we delve into the interconnection between BYSL expression and TMB, MSI, and NEO separately. The radar chart depicted that BYSL expression was positively related to the TMB of 11 cancers (CHOL, LUAD, BRCA, LGG, OV, PAAD, PRAD, LAML, READ, UCS, and SKCM) and negatively related to the TMB of KIRP, UCEC, THCA (Figure 8A). Additionally, BYSL expression displayed a significant connection to MSI in nine cancers: Positive relation to MSI in LIHC, KIRC, LUSC, BLCA, HNSC, STAD, BRCA cancers, and negative to THCA and LGG (Figure 8B). Similarly, BYSL expression positively related to NEO only in KIRC, BRCA, BLCA, and LUAD (Figure 8C).

https://doi.org/10.2147/BCTT.S537429

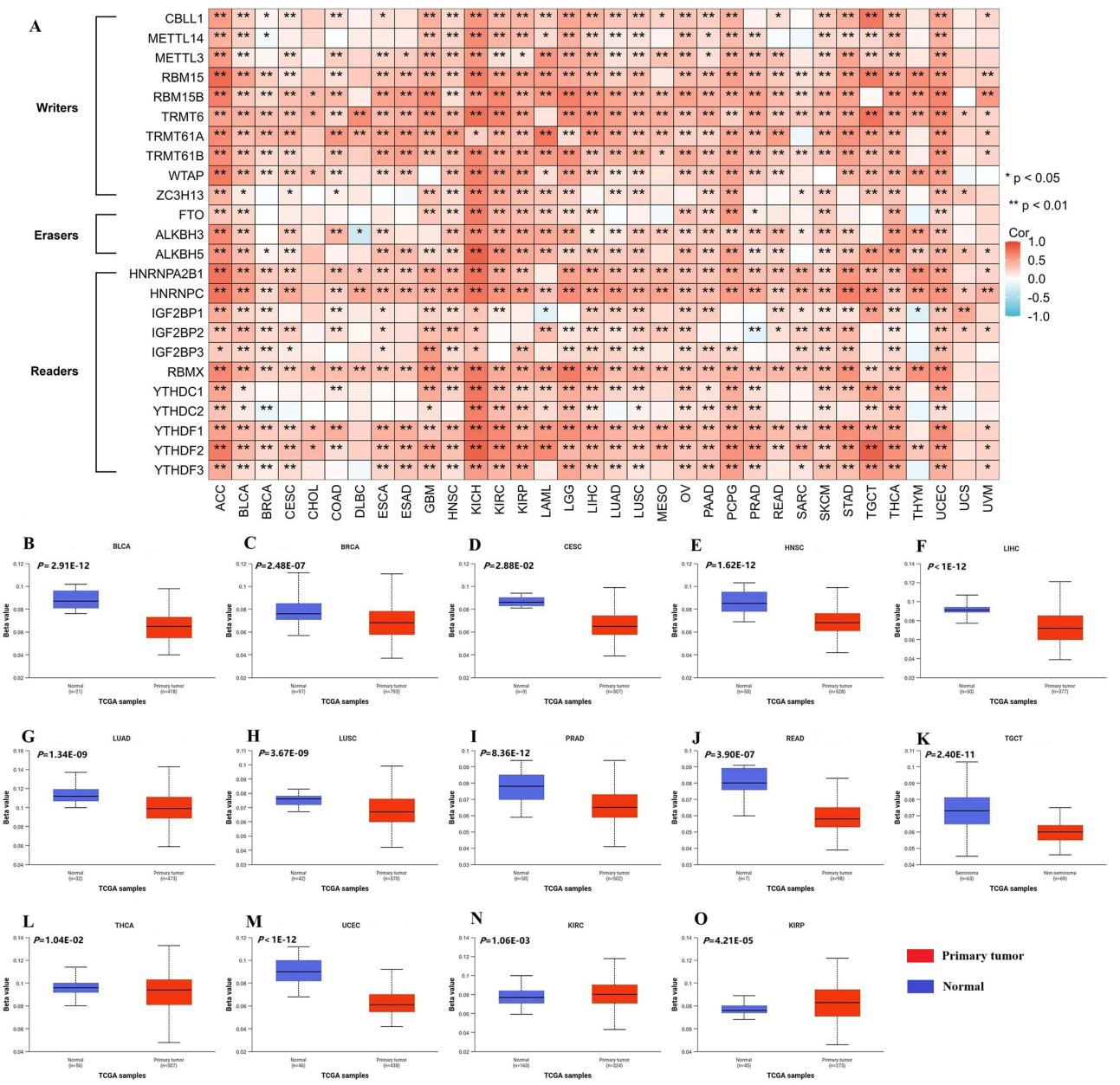

Figure 7 Epigenetic methylation analysis of BYSL. (**A**) BYSL-m6A regulator interactions across cancers. Promoter methylation level of BYSL in (**B**) BLCA, (**C**) BRCA, (**D**) CESC, (**E**) HNSC, (**F**) LIHC, (**G**) LUAD, (**H**) LUSC, (**I**) PRAD, (**J**) READ, (**K**) TGCT, (**L**) THCA, (**M**) UCEC, (**N**) KIRC, and (**O**) KIRP.

The ESTIMATE algorithm results showcased that BYSL expression was negatively linked with the stromal, immune, and ESTIMATE scores of 13 cancers (BRCA, COAD, ESCA, GBM, HNSC, LAML, LUAD, LUSC, PRAD, SARC, SKCM, STAD, and UCEC) and positively related to PCPG (Figure 8D). The correlation between BYSL expression and immune checkpoint genes (CD274, HAVCR2, LAG3, PDCD1, PDCD1LG2, TIGIT, CTLA4, and SIGLEC15) was further analyzed. The heatmap revealed that BYSL expression exhibited a negative interaction with most immune checkpoints in COAD, ESCA, GBM, LUSC, PRAD, SKCM, and THYM, whereas a positive correlation in BLCA, KICH, KIRP, and PCPG (Figure 8E).

As a key component of TME, tumor-infiltrating ICs (TIICs) are crucial in cancer treatment.[28] The results of ssGSEA revealed that the heatmap showed that among the 24 TIICs, BYSL mRNA expression was negatively related to the infiltration of B cells, cytotoxic cells, eosinophils, mast cells, iDCs, pDCs, and T cells. In contrast, it showed a significant

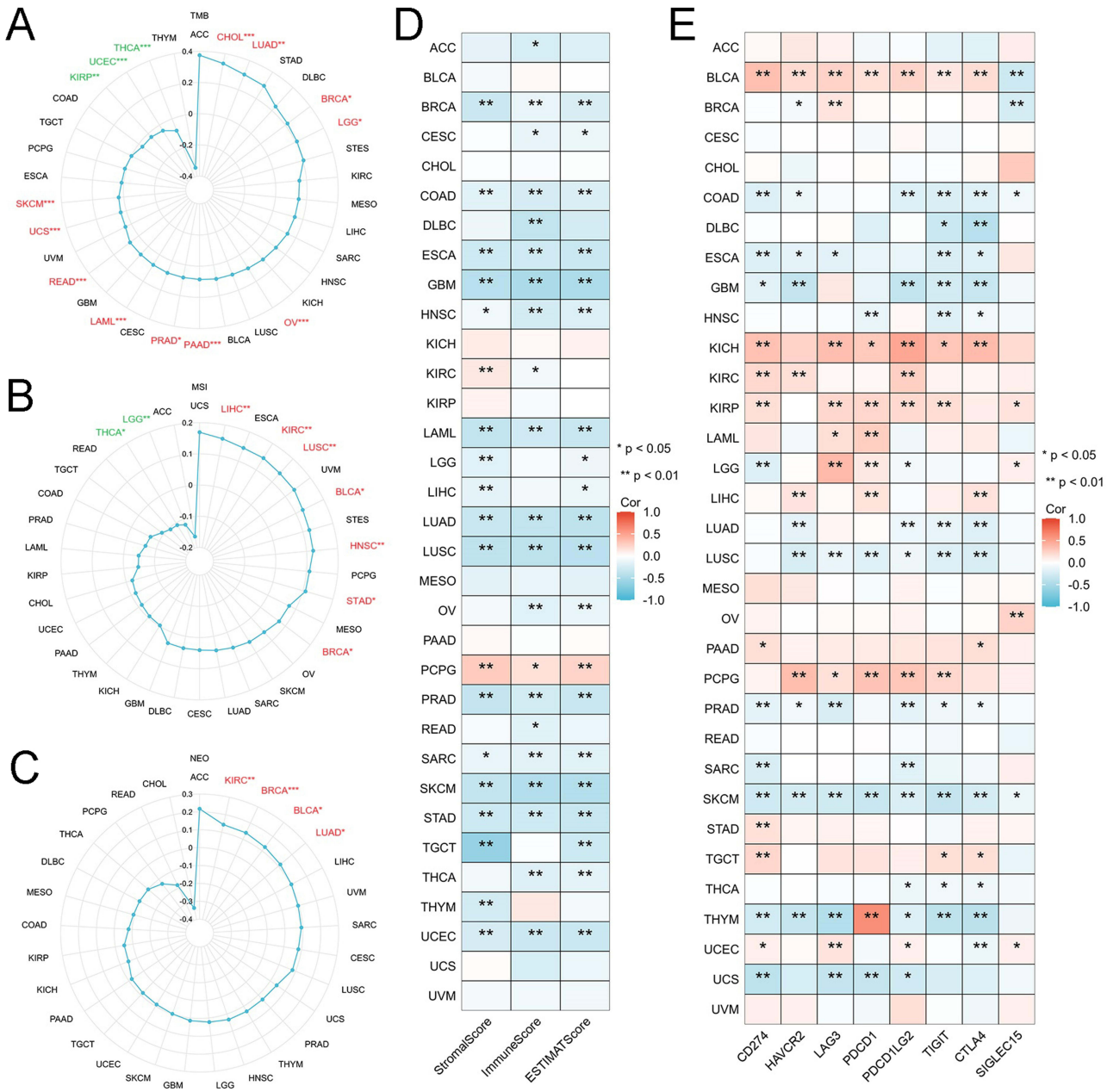

Figure 8 BYSL expression and tumor immunogenomic features. (**A**–**C**) Correlation with TMB, MSI, and NEO. (**D**) Association with TME scores. (**E**) Link to immune checkpoint expression across 33 cancers. (*p < 0.05, **p < 0.01, ***p < 0.001).

positive correlation with pro-tumor TH2 cells ($p < 0.05$), particularly in BRCA, GBM, HNSC, LUAD, PRAD, STAD, and UCEC (Figure 9A). In THYM, BYSL expression showed a positive link with CD8+/CD4+ T cells and a negative with CAF, NKs, and macrophages. In the majority of cancers, BYSL expression was significantly positively related to myeloid-derived suppressor cell (MDSC) invasion degree (Figure 9B).

Enrichment Analysis of BYSL

To investigate the molecular mechanisms underlying BYSL in cancer development, we first constructed a PPI network using 50 BYSL-binding proteins identified from the STRING database (Figure 10A). Additionally, we retrieved the top 100 BYSL co-expressed genes from the GEPIA2 database (Supplementary Table S4). A Venn diagram analysis identified

https://doi.org/10.2147/BCTT.S537429

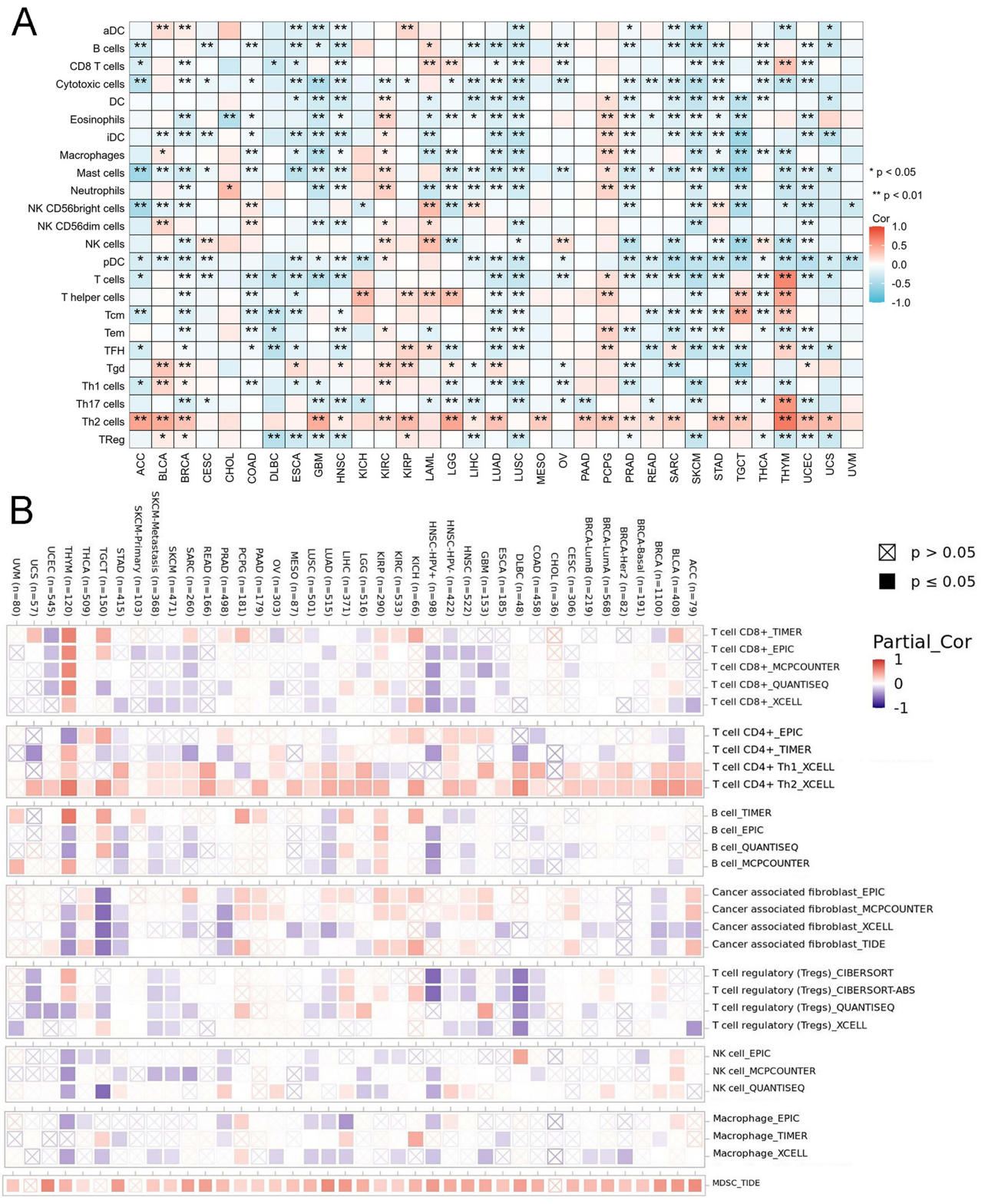

Figure 9 BYSL expression and immune cell infiltration in pan-cancer. (**A**) ssGSEA-based correlation with immune infiltration. (**B**) TIMER2.0 analysis of BYSL association with CAF infiltration.

https://doi.org/10.2147/BCTT.S537429

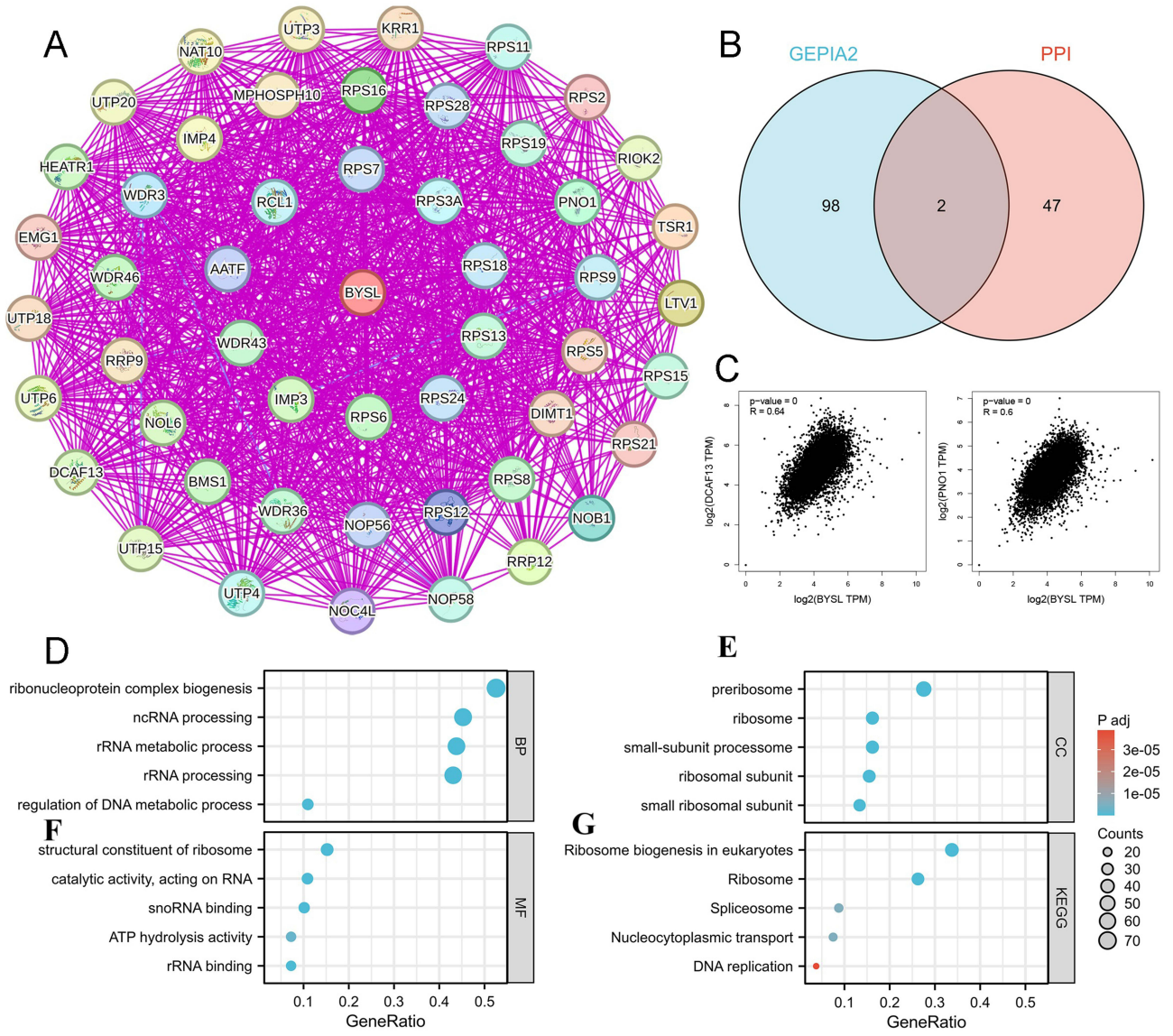

Figure 10 BYSL network, interactions, and functional enrichment. (**A**) PPI network of BYSL. (**B**) Overlapping BYSL-binding and interacting genes. (**C**) Correlation with two key genes across cancers. (**D**) GO-BP analysis. (**E**) GO-CC analysis. (**F**) GO-MF analysis. (**G**) KEGG pathway analysis.

DCAF13 and PNO1 as common genes (Figure 10B). Further correlation analysis (Figure 10C) revealed a strong positive interaction between BYSL expression and DCAF13 (r = 0.64) along with PNO1 (r = 0.60).

Furthermore, a comprehensive GO/KEGG analysis was performed,[29,30] identifying seven KEGG pathways and 225 GO categories, including 140 biological processes (BP), 45 cellular components (CC), and 40 molecular functions (MF) (Supplementary Table S3). The top five cancer-related terms for each GO category were highlighted. GO-BP analysis revealed that BYSL is involved in key BP such as ribonucleoprotein complexes biogenesis, ncRNA processing, rRNA metabolic processes, rRNA processing, regulation of DNA metabolic processes, and ribosomal biogenesis in eukaryotes (Figure 10D). GO-CC analysis showcased that BYSL-associated genes were enriched in cell components such as the pro ribosome, ribosome, small subunit processing body, ribosomal subunit, and small ribosomal subunit (Figure 10E). GO-MF analysis manifested that BYSL-related genes were potentially involved in the structural components of ribosomes, the catalytic activity of RNA, small nucleolar RNA (snoRNA) binding, adenosine triphosphate (ATP) hydrolysis activity, rRNA binding, and other MF (Figure 10F). Our KEGG pathway analysis suggests that BYSL may function by mediating pathways such as ribosomal biogenesis, ribosomes, spliceosomes, nucleocytoplasmic transport, and DNA replication in eukaryotes (Figure 10G).

https://doi.org/10.2147/BCTT.S537429

Finally, to investigate the potential BYSL-related pathways in nine cancers (BRCA, HNSC, KIRP, LIHC, LUAD, OV, SKCM, STAD, UCEC), we performed GSEA analysis, showing that genes positively linked with BYSL expression were mainly enriched in mRNA Splicing Minor Pathway, Diseases of DNA Repair and the Sumoylation of diverse proteins (DNA Damage Response and Repair Proteins, Ubiquitinylation Proteins, RNA Binding Proteins, Sumoylation Proteins and DNA Replication Proteins) (Figure 11). The genes that are negatively correlated with BYSL expression are mainly enriched in a variety of substance metabolism (the metabolism of glycogen, fatty acids, ketone bodies, amino acids, and their derivatives) and immune-related pathways (immunoregulatory interactions between a lymphoid and a non-lymphoid, signaling by the B cell receptor BCR, chemokine receptors bind chemokines and PD-1 signaling) (Supplementary Figure S6).

Collectively, BYSL is important in cancer by influencing BP such as post-transcriptional processing, DNA damage, cellular function regulation, Sumoylation modification of various proteins, cellular senescence, and immunoregulation.

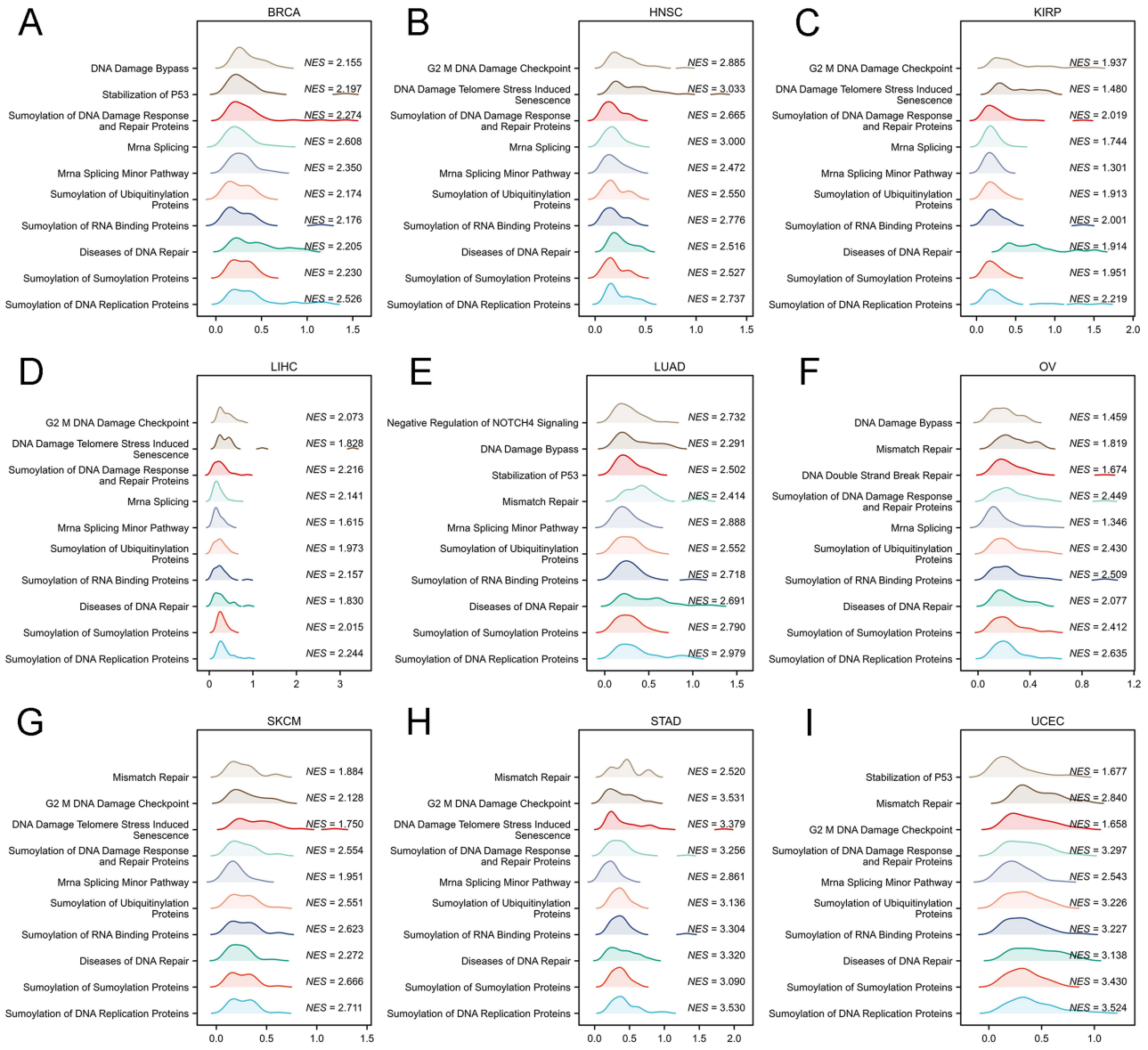

Figure 11 GSEA functional enrichment analysis of BYSL in eight cancers. In BRCA (**A**), HNSC (**B**), KIRP (**C**), LIHC (**D**), LUAD (**E**), OV (**F**), SKCM (**G**), STAD (**H**), and UCEC (**I**), the first ten pathways are positively related to BYSL expression.

Expression of BYSL in BRCA Tissues, Prognosis and Regulation of Cancer Cell Phenotype

The qRT-PCR and WB assays showcased that BYSL was significantly overexpressed in BRCA tissues (Figure 12A and B). IHC staining of paired tissue microarrays containing 80 BRCA patients showed that BYSL was overexpressed in cancer tissues compared to adjacent tissues (Figure 12C and D), which often predicted a worse prognosis (Figure 12E). To verify BRCA cell phenotype regulation by different BYSL expression levels, BYSL knockdown (BYSL-KD) and overexpression (BYSL-OE) BRCA cell lines were constructed and then verified by qRT-PCR and WB (Figure 12F and G). The CCK-8 results showed that BYSL-KD decreased BRCA proliferation, while BYSL-OE gave the opposite result (Figure 13A and B). In addition, the Transwell invasion and migration assay results showed that BYSL-KD significantly inhibited the invasion and

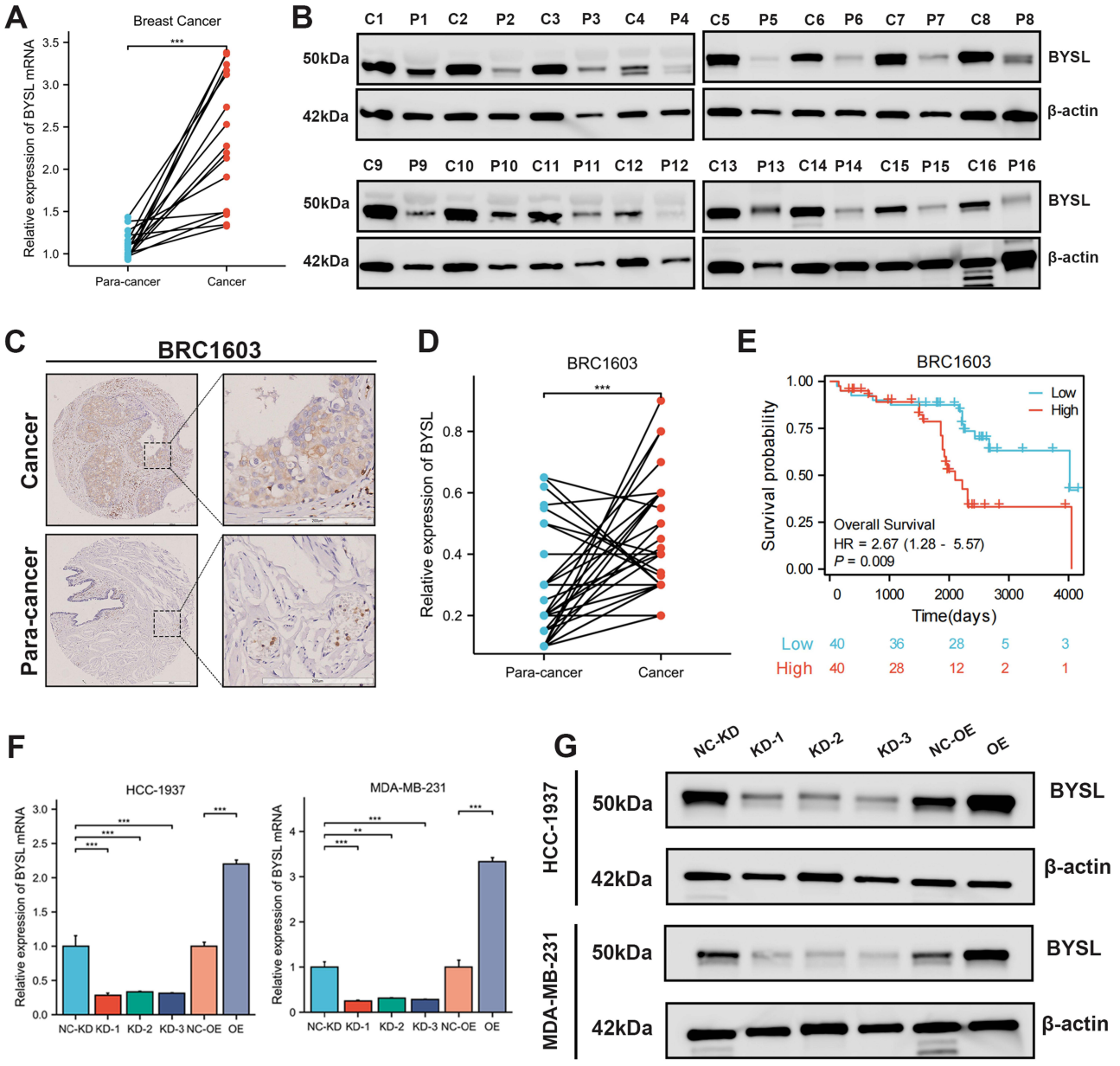

Figure 12 Expression and prognosis of BYSL in BRCA tissues, and validation of the efficiency of BYSL-KD and BYSL-OE in BRCA cells. (**A** and **B**) qRT-PCR and WB: BYSL mRNA level in cancer and adjacent counterparts of 16 BRCA patients. (**C**) IHC staining: Cancer and adjacent counterparts of BRCA patients by tissue microarrays. (**D**) Expression of BYSL in BRCA and adjacent tissues in tissue microarrays. (**E**) K-M: OS curves for high- and low-BYSL expression patients. (**F** and **G**) qRT-PCR and WB: BYSL-KD and BYSL-OE efficiency in BRCA cells. (*$p < 0.05$, **$p < 0.01$, ***$p < 0.001$).

https://doi.org/10.2147/BCTT.S537429

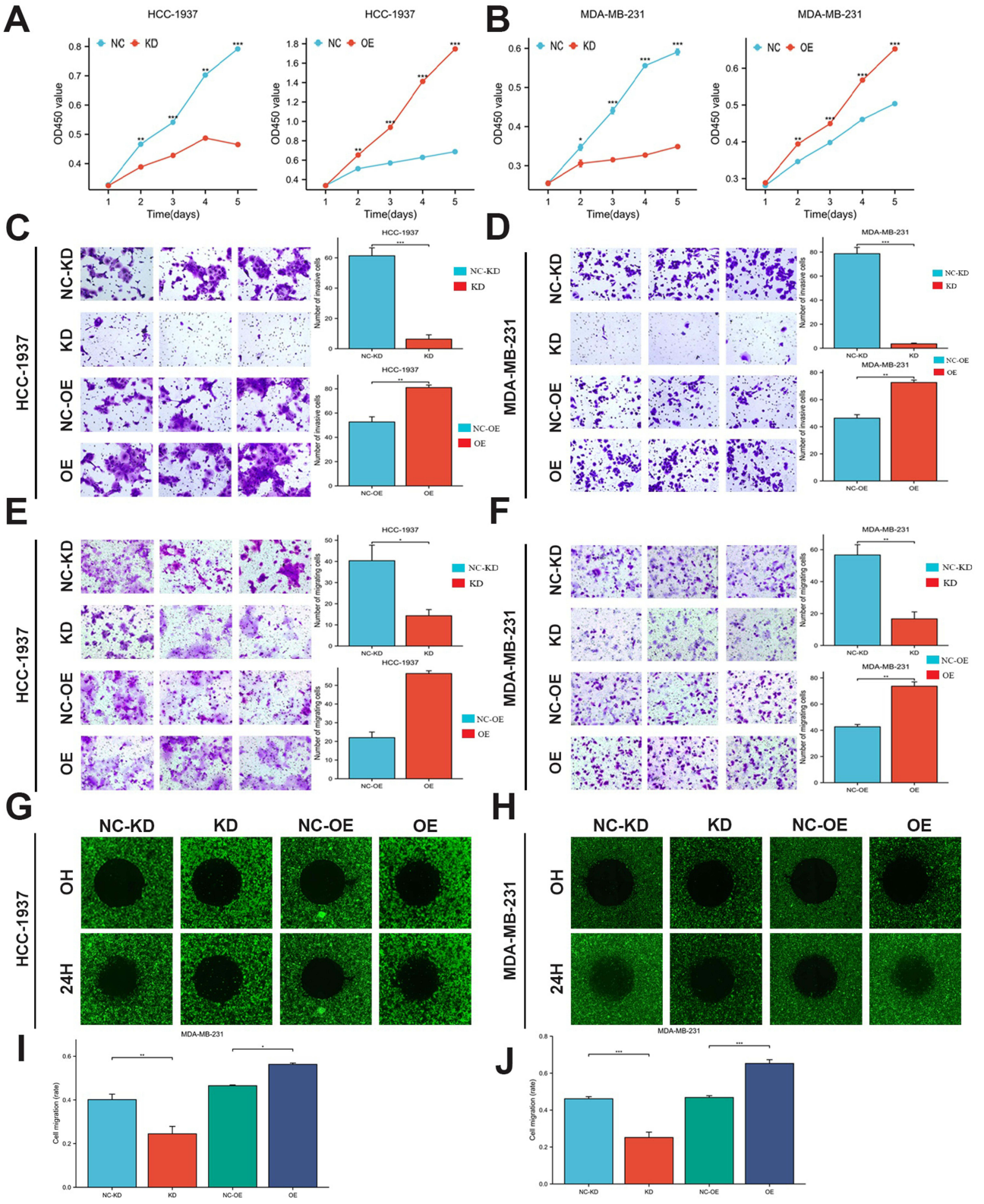

Figure 13 Effect of BYSL-KD and BYSL-OE on BRCA proliferation, invasion, and migration. (**A** and **B**) CCK-8 assay: Changes in BRCA cell lines (HCC-1937 and MDA-MB-231) proliferation after BYSL-KD and BYSL-OE, respectively. (**C** and **D**) Trans well invasion assay: Changes in BRCA cell line invasion after BYSL-KD and BYSL-OE. (**E** and **F**) Trans well migration assay: BRCA cell line migration after BYSL-KD and BYSL-OE. (**G–J**) Oris cell migration assay: Changes in BRCA cell line migration after BYSL-KD and BYSL-OE. (*p < 0.05, **p < 0.01, ***p < 0.001).

https://doi.org/10.2147/BCTT.S537429

migration of BRCA cell lines, while BYSL-OE promoted invasion and migration (Figure 13C–F). Subsequent Oris cell migration experiments re-validated the ability of BYSL-KD to inhibit the migration of BRCA cell lines, while BYSL-OE was the opposite (Figure 13G–J). In conclusion, BYSL overexpression in BRCA tissues is an important risk factor affecting the prognosis of BRCA patients. BYSL overexpression significantly promotes BRCA cell line proliferation, invasion, and migration, while low expression is the opposite.

Discussion

To our knowledge, this is the first pan-cancer study conducted on BYSL, clarifying its expression patterns and biological functions in pan-cancer to identify potential targets for new cancer diagnosis, treatment, and prognosis assessment.

BYSL, located on chromosome 6p21.1, encodes the bystin protein. Alterations in the 6p chromosomal region have been observed in malignant tumors, including osteosarcoma and renal cell carcinoma.[31,32] Our study found that BYSL was significantly overexpressed in most malignancies, unlike normal tissues, and was strongly related to poor prognosis in pan-cancer patients, especially in BRCA, COAD, HNSC, KIRP, LIHC, LUAD, OV, SKCM, and UCEC. Zhang et al showed that BYSL expression affects OS in SKCM patients, consistent with our findings. However, the enhanced BYSL expression found in their study was associated with a higher tumor stage in SKCM patients, which is different from the results of this study.[15] We observed that in SKCM patients, BYSL expression decreased with increasing clinic pathologic stage. Additionally, BYSL was overexpressed in the advanced clinicopathologic stage of ACC, KIRP, LIHC, and LUAD relative to the early stage, suggesting that BYSL may affect the prognosis of these cancer patients. High BYSL expression is positively linked with the histological grade of LIHC patients and the TNM stage of osteosarcoma patients,[7,10] which is consistent with our findings. In addition, our study found that high BYSL expression is an independent prognostic factor for OV patients, and high BYSL expression has a positive effect on patient prognosis. It should be noted that this finding shows certain differences from other research results we have observed. Currently, research on the correlation between BYSL and the prognosis of OV patients remains scarce. Therefore, in-depth exploration of the association between the two, as well as the specific mechanisms underlying opposite results in relevant studies, will be the focus of our subsequent research. In conclusion, BYSL may represent a marker for the poor prognosis of the above-mentioned cancer patients, although its prognostic value should be explored.

Herein, we employed clinical tissue samples to further verify the BYSL levels in paired BRCA samples, and their mRNA and protein levels were significantly increased compared to adjacent tissues.

Related research, through model-building, has found that BYSL overexpression promotes the tumorigenesis of HCC. Moreover, the risk score composed of BYSL and other factors can be a predictor of the prognosis of patients with gastric cancer and soft tissue sarcoma.[8,13,33] Our study found that BYSL may be a diagnostic marker for various cancers and identified BYSL as an independent PF for patients with BRCA, HNSC, KICH, LIHC, OV, and SARC, providing a theoretical basis for its application in future cancer treatment and management.

One of the hallmarks of cancer is epigenomic dysregulation, in which changes in gene expression affect the cellular state, interfere with the interaction between cells and the TME, and ultimately contribute to cancer development and progression.[34,35] This study found that BYSL mutations were present in most cancer types, BYSL mutations were positively correlated with BYSL mRNA expression levels, and high expression of BYSL mRNA results in poor prognosis in patients with various cancers. In most cancers, due to the amplification mutation of BYSL and its high-level expression of BYSL mRNA, patients with various cancers have a poor prognosis. From this, we speculate that the amplification mutation of BYSL is an important cause of the increased expression level of BYSL mRNA, leading to a poor prognosis for patients with various cancers. This is particularly evident in patients with KIRP, LIHC, and UCEC, among others. Thus, BYSL mutation is highly likely to be crucial in cancer occurrence and development. Although we are the first to systematically elucidate the important role of BYSL mutations in pan-cancer, further research should cover the mechanisms by which BYSL mutations affect cancer occurrence and progression.

As biomarkers for predicting ICI efficacy, both TMB and MSI can evaluate elements related to tumor and host immunogenicity. This provides a strong basis for formulating and optimizing clinical ICI treatment plans.[36,37] Then, we ascertained the interconnection between BYSL expression and TMB, MSI, and NEO, showing that BYSL expression in COAD, ESCA, GBM, LUSC, PRAD, and SKCM was inversely correlated with immunological scores and the expression

of most immune checkpoints. Since BYSL was overexpressed in these tumors, it may cause poor prognosis in patients with these cancers by decreasing tumor immune scores and suppressing immune-associated gene activation in these cancers. In addition, we found that BYSL expression was positively related to the three scores of BRCA, LUAD, BLCA, and KIRC and that BYSL mRNA was overexpressed in the above-mentioned cancers. Consequently, patients having BYSL overexpression in the above-mentioned cancers displayed higher immune scores and would respond better to immunotherapy. Accordingly, BYSL may contribute to cancer immunity regulation, and targeting BYSL may be a new strategy for tumor immunotherapy.

Cancer onset and development are synchronized with the remodeling of the surrounding matrix.[38] Multiple studies have shown that TME is mainly composed of tumor cells, ICs, signaling molecules, stromal tissues, and vascular systems, which promote tumor progression.[39] The expression of BYSL is inversely correlated with most ICs, mainly B cells, iDCs, pDCs, and T cells. MDSCs are considered to be the major immunosuppressive factors in the TME, using multiple effector molecules and signaling pathways to modulate immunosuppression and thus promote cancer growth.[40] In this study, BYSL expression was positively related to MDSCs. Therefore, we speculated that BYSL mainly exerts an immunosuppressive role rather than immune escape, which in turn affects the prognosis of cancer patients. As two key subsets of Th cells, Th1 and Th2 cells, exist in relative equilibrium by secreting cytokines, and their imbalance is a decisive factor in malignancy development,[41] we found that BYSL was more correlated withTh2 cells than with Th1 cells, suggesting that in the case of high expression of BYSL mRNA, the immune response has the potential to shift from exerting anti-tumor effects to promoting tumor growth.

m6A methylation is critical in governing tumor immunity and modulating proliferation, invasion, and metastasis.[42,43] This study explored the correlation between BYSL expression and methylation levels of BYSL promoters and expression of m6A methylation-related regulators. Here, BYSL expression is positively related to m6A methylation-related regulator expression in most malignancies, with ACC, BLCA, KICH, THCA, and UCEC showing an extremely strong positive correlation, suggesting that BYSL may exhibit elevated m6A methylation levels in these cancers. Disruptions in the regulatory mechanisms of DNA methylation can result in a variety of diseases, including cancer.[44] Previous studies have shown that BYSL expression is negatively governed by BYSL methylation. Our analysis showed that BYSL hypermethylation was related to an improved KIRC prognosis and a worsening BLCA prognosis, thus highlighting the important role of BYSL methylation in cancer initiation and progression.

The progression of cancer depends on the biogenesis of ribosomes, and the nucleolus is an important organelle for ribosomal biogenesis.[45] Bystin is located in the nucleolus and is related to the cytoplasmic 40S subunit pre-translation. Its downregulation delays 18S rRNA processing, the mature form required for protein translation, resulting in impaired cell viability.[46] BYSL has been shown to mediate the activation of related protein kinases through mTOR, GSK-3β/β-catenin, and other signalings, thereby promoting glioma cell proliferation, invasion, and migration.[47,48] BYSL silencing leads to cell cycle arrest and an increase in long-term OS, which is consistent with our findings.[49]

Our analysis find that BYSL may contribute to Sumoylation modification of various proteins, cellular senescence, and immune regulation. Furthermore, We speculate that BYSL may be involved in the P53 stabilization process. However, it should be noted that this association is only a theoretical speculation, as this study has not verified it experimentally. Thus, it could serve as a direction for future research, and its specific mechanism remains to be further explored. Among them, p53 is one of the most widely studied tumor suppressors, and its loss or mutation of function is closely linked with cancer occurrence and progression.[49] P53 stabilization maintains genomic stability and inhibits tumorigenesis. However, the specific mechanism behind BYSL in cancer occurrence and progression remains vague. Therefore, our cell experiments validated that BYSL-KD can inhibit BRCA cell proliferation, invasion, and migration and increase apoptosis, providing new insight into the role of BYSL and the development of innovative cancer therapies.

Conclusion

This is the first systematic study of BYSL at the pan-cancer level through bioinformatics analysis. Our findings demonstrate that BYSL may drive tumor progression by regulating ribosomal biosynthesis and cell cycle-associated signaling pathways. Through expression and functional validation experiments in BRCA, we further validated its role in tumorigenesis and development. Collectively, our study establishes BYSL as a potential diagnostic and prognostic

biomarker, as well as a therapeutic target, for human cancers. Future investigations are warranted to further elucidate its molecular mechanisms and explore clinical translation.

Abbreviations

BLCA, Bladder Urothelial Carcinoma; BRCA, Breast Cancer; BYSL-KD, BYSL Knockdown; OE, Overexpression; CESC, Cervical squamous cell carcinoma and endocervical adenocarcinoma; CHOL, Cholangiocarcinoma; CNV, Copy Number Variants; COAD, Colon adenocarcinoma; DLBC, Lymphoid Neoplasm Diffuse Large B-cell Lymphoma; DSS, Disease-specific Survival; ESCA, Esophageal carcinoma; GBM, Glioblastoma multiforme; HNSC, Head and neck squamous cell carcinoma; IHC, Immunohistochemistry; KICH, Kidney chromophobe cell carcinoma; KIRC, Kidney renal clear cell carcinoma; KIRP, Kidney renal papillary cell carcinoma; K-M, Kaplan-Meier; LAML, Acute Myeloid Leukemia; LGG, Brain Lower Grade Glioma; LIHC, Liver hepatocellular carcinoma; LUAD, Lung adenocarcinoma; LUSC, Lung squamous cell carcinoma; MSI, Microsatellite Instability; NEO, Neoantigen; OS, Overall Survival; OV, Ovarian serous cystadenocarcinoma; PAAD, Pancreatic adenocarcinoma; PFS, Progression-free Survival; PPI, Protien-protien Interaction; PRAD, Prostate adenocarcinoma; READ, Rectum adenocarcinoma; SKCM, Skin Cutaneous Melanoma; STAD, Stomach adenocarcinoma; TGCT, Testicular Germ Cell Tumors; THYM, Thymoma; TMB, Tumor Mutational Burden; TME Tumor Microenvironment; UCEC, Uterine corpus endometrial carcinoma; UCS, Uterine Carcinosarcoma; WB, Western blotting.

Data Sharing Statement

The article/supplementary material includes the original contributions. For further inquiries, please contact the corresponding author.

Ethics Statement

Our study complies with the Declaration of Helsinki, The First Affiliated Hospital of Xinjiang Medical University Ethics Committee authorized the studies involving humans (No. 230714-08) that followed local legislation and institutional guidelines. The participants signed informed consent before participation.

Author Contributions

All authors made a significant contribution to the work reported, whether that is in the conception, study design, execution, acquisition of data, analysis and interpretation, or in all these areas; took part in drafting, revising or critically reviewing the article; gave final approval of the version to be published; have agreed on the journal to which the article has been submitted; and agree to be accountable for all aspects of the work. Xiyidan Aimaiti, Yiyang Wang, and Dilimulati Ismtula made equal contributions to this work and shared the first authorship.

Funding

State Key Laboratory of Pathogenesis, Prevention, Treatment of Central Asian High Incidence Diseases Fund (SKL-HIDCA-2024-21), National Natural Science Foundation of China (32260186), Xinjiang Uygur Autonomous Region Youth Science and Technology Top-notch Talent Program (2022TSYCCX0029), Regional Collaborative Innovation Special Project (Science and Technology Assistance to Xinjiang Program) (2022E02136), National Health Commission of the People's Republic of China (WKZX2023WK0109), Outstanding Youth Science Fund (2024D01E22).

Disclosure

The authors report no conflicts of interest in this work.

References

1. Huq MS, Acharya SC, Gautam M, et al. Cancer research in South Asian Association for Regional Cooperation (SAARC) countries. *Lancet Oncol*. 2024;25(12):e675–e684. doi:10.1016/S1470-2045(24)00518-7

2. Jokhadze N, Das A, Dizon DS. Global cancer statistics: a healthy population relies on population health. *CA Cancer J Clin*. 2024;74(3):224–226. doi:10.3322/caac.21838
3. Zhang A, Miao K, Sun H, Deng CX. Tumor heterogeneity reshapes the tumor microenvironment to influence drug resistance. *Int J Biol Sci*. 2022;18(7):3019–3033. doi:10.7150/ijbs.72534
4. Carron C, O'Donohue MF, Choesmel V, Faubladier M, Gleizes PE. Analysis of two human pre-ribosomal factors, bystin and hTsr1, highlights differences in evolution of ribosome biogenesis between yeast and mammals. *Nucleic Acids Res*. 2011;39(1):280–291. doi:10.1093/nar/gkq734
5. Ishikawa H, Yoshikawa H, Izumikawa K, et al. Poly(A)-specific ribonuclease regulates the processing of small-subunit rRNAs in human cells. *Nucleic Acids Res*. 2017;45(6):3437–3447. doi:10.1093/nar/gkw1047
6. Miyoshi M, Okajima T, Matsuda T, Fukuda MN, Nadano D. Bystin in human cancer cells: intracellular localization and function in ribosome biogenesis. *Biochem J*. 2007;404(3):373–381. doi:10.1042/BJ20061597
7. Sun J, Li Y, Tian H, Chen H, Li J, Li Z. Comprehensive analysis identifies long non-coding RNA RNASEH1-AS1 as a potential prognostic biomarker and oncogenic target in hepatocellular carcinoma. *Am J Cancer Res*. 2024;14(3):996–1014. doi:10.62347/JPHF4071
8. Wang H, Xiao W, Zhou Q, et al. Bystin-like protein is upregulated in hepatocellular carcinoma and required for nucleologenesis in cancer cell proliferation. *Cell Res*. 2009;19(10):1150–1164. doi:10.1038/cr.2009.99
9. Wu Y, Chen X, Zhao Y, Wang Y, Li Y, Xiang C. Genome-wide DNA methylation and hydroxymethylation analysis reveal human menstrual blood-derived stem cells inhibit hepatocellular carcinoma growth through oncogenic pathway suppression via regulating 5-hmC in enhancer elements. *Stem Cell Res Ther*. 2019;10(1):151. doi:10.1186/s13287-019-1243-8
10. Zhang J, Tang H, Jiang X, Huang N, Wei Q. Hypoxia-induced miR-378a-3p inhibits osteosarcoma invasion and epithelial-to-mesenchymal transition via BYSL regulation. *Front Genet*. 2021;12:804952. doi:10.3389/fgene.2021.804952
11. Ochnik AM, Peterson MS, Avdulov SV, Oh AS, Bitterman PB, Yee D. Amplified in breast cancer regulates transcription and translation in breast cancer cells. *Neoplasia*. 2016;18(2):100–110. doi:10.1016/j.neo.2016.01.001
12. Ayala GE, Dai H, Li R, et al. Bystin in perineural invasion of prostate cancer. *Prostate*. 2006;66(3):266–272. doi:10.1002/pros.20323
13. Ning ZK, Tian HK, Liu J, et al. Analysis and application of RNA binding protein gene pairs to predict the prognosis of gastric cancer. *Heliyon*. 2023;9(7):e18242. doi:10.1016/j.heliyon.2023.e18242
14. Godoy H, Mhawech-Fauceglia P, Beck A, et al. Developmentally restricted differentiation antigens are targets for immunotherapy in epithelial ovarian carcinoma. *Int J Gynecol Pathol*. 2013;32(6):536–540. doi:10.1097/PGP.0b013e318275a550
15. Wang ZZ, Yao GT, Wang LZ, Zhu YJ, Chen JH. Increased expression and prognostic significance of BYSL in melanoma. *J Immunother*. 2024;47(8):279–302. doi:10.1097/CJI.0000000000000530
16. Chandrashekar DS, Karthikeyan SK, Korla PK, et al. UALCAN: an update to the integrated cancer data analysis platform. *Neoplasia*. 2022;25:18–27. doi:10.1016/j.neo.2022.01.001
17. Thul PJ, Lindskog C. The human protein atlas: a spatial map of the human proteome. *Protein Sci*. 2018;27(1):233–244. doi:10.1002/pro.3307
18. Gyorffy B. Integrated analysis of public datasets for the discovery and validation of survival-associated genes in solid tumors. *Innovation*. 2024;5(3):100625. doi:10.1016/j.xinn.2024.100625
19. Gao J, Aksoy BA, Dogrusoz U, et al. Integrative analysis of complex cancer genomics and clinical profiles using the cBioPortal. *Sci Signal*. 2013;6(269):pl1. doi:10.1126/scisignal.2004088
20. Liu CJ, Hu FF, Xie GY, et al. GSCA: an integrated platform for gene set cancer analysis at genomic, pharmacogenomic and immunogenomic levels. *Brief Bioinform*. 2023;24(1). doi:10.1093/bib/bbac558
21. Chen D, Xu L, Xing H, et al. Sangerbox 2: enhanced functionalities and update for a comprehensive clinical bioinformatics data analysis platform. *Imeta*. 2024;3(5):e238. doi:10.1002/imt2.238
22. Li T, Fu J, Zeng Z, et al. TIMER2.0 for analysis of tumor-infiltrating immune cells. *Nucleic Acids Res*. 2020;48(W1):W509–W514. doi:10.1093/nar/gkaa407
23. Szklarczyk D, Kirsch R, Koutrouli M, et al. The STRING database in 2023: protein-protein association networks and functional enrichment analyses for any sequenced genome of interest. *Nucleic Acids Res*. 2023;51(D1):D638–D646. doi:10.1093/nar/gkac1000
24. Tang Z, Kang B, Li C, Chen T, Zhang Z. GEPIA2: an enhanced web server for large-scale expression profiling and interactive analysis. *Nucleic Acids Res*. 2019;47(W1):W556–W560. doi:10.1093/nar/gkz430
25. Liberzon A, Birger C, Thorvaldsdottir H, Ghandi M, Mesirov JP, Tamayo P. The Molecular Signatures Database (MSigDB) hallmark gene set collection. *Cell Syst*. 2015;1(6):417–425. doi:10.1016/j.cels.2015.12.004
26. Landolt L, Spagnoli GC, Hertig A, Brocheriou I, Marti HP. Fibrosis and cancer: shared features and mechanisms suggest common targeted therapeutic approaches. *Nephrol Dial Transplant*. 2022;37(6):1024–1032. doi:10.1093/ndt/gfaa301
27. Nishiyama A, Nakanishi M. Navigating the DNA methylation landscape of cancer. *Trends Genet*. 2021;37(11):1012–1027. doi:10.1016/j.tig.2021.05.002
28. Vishwakarma S, Arya N, Kumar A. Regulation of tumor immune microenvironment by sphingolipids and lysophosphatidic acid. *Curr Drug Targets*. 2022;23(6):559–573. doi:10.2174/1389450122666211208111833
29. Kanehisa M, Goto S. KEGG: kyoto encyclopedia of genes and genomes. *Nucleic Acids Res*. 2000;28(1):27–30. doi:10.1093/nar/28.1.27
30. Kanehisa M, Sato Y, Kawashima M, Furumichi M, Tanabe M. KEGG as a reference resource for gene and protein annotation. *Nucleic Acids Res*. 2016;44(D1):D457–62. doi:10.1093/nar/gkv1070
31. Gupta S, Ito T, Alex D, et al. RUNX2 (6p21.1) amplification in osteosarcoma. *Hum Pathol*. 2019;94:23–28. doi:10.1016/j.humpath.2019.09.010
32. Gupta S, Johnson SH, Vasmatzis G, et al. TFEB-VEGFA (6p21.1) co-amplified renal cell carcinoma: a distinct entity with potential implications for clinical management. *Mod Pathol*. 2017;30(7):998–1012. doi:10.1038/modpathol.2017.24
33. Lin LL, Liu ZZ, Tian JZ, et al. Integrated analysis of nine prognostic RNA-binding proteins in soft tissue Sarcoma. *Front Oncol*. 2021;11:633024. doi:10.3389/fonc.2021.633024
34. Hanahan D. Hallmarks of cancer: new dimensions. *Cancer Discov*. 2022;12(1):31–46. doi:10.1158/2159-8290.CD-21-1059
35. Hogg SJ, Beavis PA, Dawson MA, Johnstone RW. Targeting the epigenetic regulation of antitumour immunity. *Nat Rev Drug Discov*. 2020;19(11):776–800. doi:10.1038/s41573-020-0077-5
36. Qin Y, Huo M, Liu X, Li SC. Biomarkers and computational models for predicting efficacy to tumor ICI immunotherapy. *Front Immunol*. 2024;15:1368749. doi:10.3389/fimmu.2024.1368749

37. Tan S, Day D, Nicholls SJ, Segelov E. Immune checkpoint inhibitor therapy in oncology: current uses and future directions: JACC: CardioOncology state-of-the-art review. *JACC CardioOncol*. 2022;4(5):579–597. doi:10.1016/j.jaccao.2022.09.004
38. Hinshaw DC, Shevde LA. The tumor microenvironment innately modulates cancer progression. *Cancer Res*. 2019;79(18):4557–4566. doi:10.1158/0008-5472.CAN-18-3962
39. Jin Y, Huang Y, Ren H, et al. Nano-enhanced immunotherapy: targeting the immunosuppressive tumor microenvironment. *Biomaterials*. 2024;305:122463. doi:10.1016/j.biomaterials.2023.122463
40. Li T, Liu T, Zhu W, et al. Targeting MDSC for immune-checkpoint blockade in cancer immunotherapy: current progress and new prospects. *Clin Med Insights Oncol*. 2021;15:11795549211035540. doi:10.1177/11795549211035540
41. Shang Q, Yu X, Sun Q, Li H, Sun C, Liu L. Polysaccharides regulate Th1/Th2 balance: a new strategy for tumor immunotherapy. *Biomed Pharmacother*. 2024;170:115976. doi:10.1016/j.biopha.2023.115976
42. Li Y, Jin H, Li Q, Shi L, Mao Y, Zhao L. The role of RNA methylation in tumor immunity and its potential in immunotherapy. *Mol Cancer*. 2024;23(1):130. doi:10.1186/s12943-024-02041-8
43. Mu S, Zhao K, Zhong S, Wang Y. The role of m6A methylation in tumor immunity and immune-associated disorder. *Biomolecules*. 2024;14(8). doi:10.3390/biom14081042
44. Huang W, Li H, Yu Q, Xiao W, Wang DO. LncRNA-mediated DNA methylation: an emerging mechanism in cancer and beyond. *J Exp Clin Cancer Res*. 2022;41(1):100. doi:10.1186/s13046-022-02319-z
45. Pecoraro A, Pagano M, Russo G, Russo A. Ribosome biogenesis and cancer: overview on ribosomal proteins. *Int J Mol Sci*. 2021;22(11). doi:10.3390/ijms22115496
46. Zemp I, Wandrey F, Rao S, et al. CK1delta and CK1epsilon are components of human 40S subunit precursors required for cytoplasmic 40S maturation. *J Cell Sci*. 2014;127(Pt 6):1242–1253. doi:10.1242/jcs.138719
47. Gao S, Sha Z, Zhou J, et al. BYSL contributes to tumor growth by cooperating with the mTORC2 complex in gliomas. *Cancer Biol Med*. 2021;18(1):88–104. doi:10.20892/j.issn.2095-3941.2020.0096
48. Sha Z, Zhou J, Wu Y, et al. BYSL promotes glioblastoma cell migration, invasion, and mesenchymal transition through the GSK-3beta/beta-catenin signaling pathway. *Front Oncol*. 2020;10:565225. doi:10.3389/fonc.2020.565225
49. Huang J. Current developments of targeting the p53 signaling pathway for cancer treatment. *Pharmacol Ther*. 2021;220:107720. doi:10.1016/j.pharmthera.2020.107720